PCCP

ROYAL SOCIETY OF CHEMISTRY

REVIEW

View Article Online
View Journal

Cite this: DOI: 10.1039/d3cp06142f

Advances in nanofluidic field-effect transistors: external voltage-controlled solid-state nanochannels for stimulus-responsive ion transport and beyond

G. Laucirica, †*[a] Y. Toum-Terrones, [a] V. M. Cayón,[c] M. E. Toimil-Molares,[bc] O. Azzaroni [a] and W. A. Marmisollé *[a]

Received 18th December 2023,
Accepted 20th February 2024

DOI: 10.1039/d3cp06142f

rsc.li/pccp

Ion channels, intricate protein structures facilitating precise ion passage across cell membranes, are pivotal for vital cellular functions. Inspired by the remarkable capabilities of biological ion channels, the scientific community has ventured into replicating these principles in fully abiotic solid-state nanochannels (SSNs). Since the gating mechanisms of SSNs rely on variations in the physicochemical properties of the channel surface, the modification of their internal architecture and chemistry constitutes a powerful strategy to control the transport properties and, consequently, render specific functionalities. In this framework, both the design of the nanofluidic platform and the subsequent selection and attachment of different building blocks gain special attention. Similar to biological ion channels, functional SSNs offer the potential to finely modulate ion transport in response to various stimuli, leading to innovations in a variety of fields. This comprehensive review delves into the intricate world of ion transport across stimuli-responsive SSNs, focusing on the development of external voltage-controlled nanofluidic devices. This kind of field-effect nanofluidic technology has attracted special interest due to the possibility of real-time reconfiguration of the ion transport with a non-invasive strategy. These properties have found interesting applications in drug delivery, biosensing, and nanoelectronics. This document will address the fundamental principles of ion transport through SSNs and the construction, modification, and applications of external voltage-controlled SSNs. It will also address future challenges and prospects, offering a comprehensive perspective on this evolving field.

Introduction

Ion channels, intricate protein structures that facilitate precise ion passage across cell membranes, are indispensable for maintaining essential cellular functions.[1–4] While there is a broad nature of ion channels, some of them present interesting ion transport properties, including selectivity, sensitivity to environmental changes, and rapid response. These nanostructures are responsible for critical processes such as nerve signal transmission and cellular homeostasis. Inspired by the remarkable capabilities of biological ion channels, scientists have embarked on a quest to replicate their principles and functionalities in fully abiotic nanochannels, so-called solid-state nanochannels (SSNs).[5–7]

The transport properties of SSNs can be easily tested by placing the membrane with nanochannels between two electrolyte solution reservoirs, with electrodes connected to a potentiostat for precise control of the transmembrane voltage. Upon the application of a transmembrane voltage, ions are forced to flux through the nanochannels giving rise to an ion current. This kind of signal, where ions are the signal carriers, is typically called ''iontronic output'' in analogy to electronic signals where electrons or holes serve as signal carriers.[5,8] Beyond the matter transport across SSNs, the generation of iontronic signals is the cornerstone for the applications of this kind of device in several fields such as sensing and nanoelectronics.

The concept of ion transport control, fundamental to various biological processes and central to numerous technological applications, has been a subject of profound scientific

[a] Instituto de Investigaciones Fisicoquímicas Teóricas y Aplicadas (INIFTA), Departamento de Química, Facultad de Ciencias Exactas, Universidad Nacional de La Plata, CONICET – CC 16 Suc. 4, 1900 La Plata, Argentina.
E-mail: gregoriolaucirica@quimica.unlp.edu.ar, wmarmi@inifta.unlp.edu.ar
[b] GSI Helmholtzzentrum für Schwerionenforschung GmbH, 64291 Darmstadt, Germany
[c] Department of Materials- and Geosciences, Technical University of Darmstadt, Darmstadt, Germany
† Current address: UCAM-SENS, Universidad Católica San Antonio de Murcia, UCAM HiTech, 30107 Murcia, Spain.

interest for decades. Biological ion channels possess the remarkable ability to modulate ion transport in response to various stimuli, a feature that opens the floodgates to numerous possibilities for creating versatile platforms applied across various fields. This capability inspired the scientific community to develop SSN devices that can tune and control the movement of ions by different stimuli, harnessing the potential of responsive ion transport in diverse applications ranging from chemical fluidic actuation[9–12] to biosensing,[13–16] and from nanoelectronics to energy conversion systems.[17–22] Up to now, it is well-known that ion transport through SSNs (and consequently, iontronic output) is mainly determined by the channel geometry and the physicochemical properties of the channel surface.[23,24] For instance, if the channel aperture is in the nanometric range, the ion enrichment generated by the surface charges determines an ion transport governed by the surface charge density. Similarly, the wettability properties of the surface as well as the variations in the inner free volume of the channel can also act as efficient gating mechanisms.[25,26]

Notably, the symmetry of the channel plays also a central role in the iontronic signals. Symmetrical channels display an ohmic behavior, as the current maintains a linear relationship

G. Laucirica

Gregorio Laucirica obtained his Degree in Chemistry (2018) and PhD in Chemistry (2023) at the Universidad Nacional de La Plata (UNLP) in La Plata, Argentina. Currently, he is a postdoctoral researcher at the UCAM-SENS unit from Universidad Católica San Antonio de Murcia (UCAM) in Murcia, Spain. His research is centred on studying, developing, and characterizing electrochemical platforms based on nanodevices, with applications in (bio)sensing and nanoelectronics.

Y. Toum-Terrones

Yamili Toum studied chemistry at the University of Buenos Aires (UBA) (Argentina), receiving his PhD in 2019 for research involving the organic synthesis of tricarbocyanines and their integration into silica nanoparticles for fluorescent nanosensors. Her postdoctoral studies were carried out at the Soft Matter Laboratory at INIFTA, where she could dedicate her studies to the integration of enzymes into track-etched solid-state nanochannels. Since 2023, she has been the head of an R&D area in a pharmaceutical company in Argentina. Her research interests include biosensing of neurological disease biomarkers based on polymer track-etched nanochannels and supramolecular materials.

V. M. Cayón

Vanina Cayón studied Chemistry at the National University of La Plata (UNLP)(Argentina), where she also obtained her PhD in Chemistry in 2019. From 2019 to 2022, she was a postdoc at Soft Matter Laboratory (INIFTA-UNLP) and specialized in nanofluidic devices. She has also been a teaching assistant at UNLP from 2013 to 2022. Since 2022, she has worked as a scientist at the GSI Helmholtz Center in Darmstadt. As a member of the Materials Research Department, she participates in irradiation experiments at the GSI accelerator facilities and contributes to the design of biosensors and antiviral surfaces based on track-etched membranes.

M. E. Toimil-Molares

Maria Eugenia Toimil-Molares is since 2023 the head of the Materials Research Department of the GSI Helmholtz Center (MRD-GSI) and a professor in the Materials- and Geoscience Department of the TUD (Darmstadt, Germany). She received her MS degree in Physics at the University of Santiago de Compostela (Spain) in 1997 and a PhD degree by the Faculty of Physics and Astronomy at the University of Heidelberg (Germany) in 2001. From 2002 to 2006, she was a postdoc in the MRD-GSI. From 2007 to 2009, she worked at the University of California Berkeley (USA) as a visiting researcher and at Sandia National Laboratories in Livermore (USA). In 2009 she joined the MRD-GSI, leading an experimental group working on the fabrication of nanostructures by ion-track technology and electrodeposition, and their characterization.

with the transmembrane voltage.[5,24] Conversely, asymmetric channels evidence an ion current rectification (ICR) behavior due to the disruption of the electrical potential symmetry. The ICR transport regime is characterized by an enhancement of the ion current (fluxes) at a given transmembrane voltage polarity.[27–30] One of the simplest ways to control the symmetry of the channel is by designing channels with different geometries. However, depending on the nanofabrication method (and the material), the creation of geometrically asymmetric channels can be not trivial. For those cases, a feasible way to impart asymmetry is through the asymmetric modification of the channel surface chemistry. Additionally, the integration of different building blocks onto the channel surface with the ability to trigger any structural or charge change upon the presence of any environmental changes provides a reliable method to generate stimuli-responsive nanodevices.

Considering all of this context, it becomes evident that the control of the internal architecture and chemistry of the SSNs is the primary approach to manipulate ion transport at the nanoscale and, thus, create functional SSNs. In particular, the present review is focused on the development of SSNs with ion transport modulated by external voltages, so-called nanofluidic field-effect transistors (nFETs), or ionic FETs.[31,32] Within these systems, the membranes with nanochannels serve as the foundation upon which nFETs are built, providing a rational pathway for the precise manipulation of ion transport *via* the application of external voltages to the channel walls/membrane surface. Therefore, nFETs offer the ability to modulate ion currents and matter transport in response to a non-invasive stimulus, opening the door to a myriad of applications.

As the exploration of nFETs advances, it is essential to emphasize the construction and modification of SSNs. Various materials have been employed to construct nanofluidic devices, including silicon dioxide, alumina, and polymers, with each material offering distinct advantages and challenges.[6,25,33–35] While material selection for nanofluidic devices lays the foundation, it is the modification of the nanofluidic surface that brings nFETs to life. The crucial aspect of nFET creation revolves around the integration of materials with suitable electrical conductivity and responsiveness onto the channel walls or entrances. This integration breathes electrical responsiveness into the nanofluidic surface, enabling the application of the external voltage and localized variations in physicochemical properties.

In this comprehensive review, we will delve into the intricate world of ion transport across SSNs, with a particular focus on recent developments of nFETs. We will present shortly the fundamental principles that govern ion transport in SSNs and the construction and modification of these nanofluidic devices, and focus then on the development of SSNs nFETs. This review concentrates on SSNs (*i.e.* channel length significantly greater than tip diameter), and provides in addition a concise discussion of nFET based on solid-state nanopores (*i.e.* pore length comparable to tip diameters), which are technologically relevant for sensing purposes. We will discuss some of their wide-ranging applications and, finally, we will identify and address the challenges and prospects that lie ahead, aiming to provide a comprehensive perspective on this fascinating and rapidly evolving field.

Ion transport in solid-state nanochannels

The ion flux through SSNs is determined by the physicochemical properties of the channel surface, in particular, the orchestration of surface charge, wettability, and volume effects. While the basics of ion transport have been reported and reviewed

O. Azzaroni

Omar Azzaroni, a chemist, earned his PhD from Universidad Nacional de La Plata (Argentina) in 2004. He conducted postdoctoral research at the University of Cambridge (UK) (2004–2006) and the Max Planck Institute for Polymer Research (Germany) (2007). He led a Max Planck Partner Group from 2009 to 2013 and served as Vice-Director of INIFTA (2012–2015). Currently, he is a fellow member of CONICET, heads the Soft Matter Laboratory at INIFTA, and is a Full Professor at UNLP. His research focuses on integrating functional molecular systems into devices like solid-state nanopores, graphene-based transistors, and bioelectrochemical sensors. More details: ***https://softmatter.quimica.unlp.edu.ar****.*

W. A. Marmisollé

Waldemar Marmisolle graduated in Chemistry from the Universidad Nacional de La Plata (UNLP), Argentina, in 2007 and also completed his PhD in Chemistry at UNLP in 2011. He is a research staff member of CONICET at INIFTA and a Professor of Physical Chemistry at UNLP. His research focuses on the physicochemical aspects of electrochemical processes and the construction and characterization of electroactive materials.

elsewhere,[18,23,33] here we discuss the effects governing the gating mechanism and their subsequent transduction into readable signals.

Surface charge effects

Most of the systems that will be analyzed in this review involve the use of nanochannels with charged surfaces. The charge usually is provided by the presence of organic molecules with ionizable groups or the polarization of a metal surface. For instance, after nanofabrication, nanofluidic devices based on track-etched or aluminum oxide membranes exhibit acid–base surface groups capable to acquire a net charge at certain pH conditions. In other cases, molecular systems with ionizable groups, including polyelectrolytes, organosilanes, polymer brushes, biomolecules, *etc.*, can be incorporated onto the channel walls (or membrane surface) by employing different chemical or physical routes. Beyond the specific origin of the surface charges, this scenario requires an understanding of the interactions between charged surfaces and an electrolytic solution.

The immersion of a charged surface in an electrolyte solution triggers an ion redistribution in the proximity of the surface. In honor of the first models proposed to explain and characterize this phenomenon, the surrounding solution area is called the electrical double layer (EDL). Considering only electrostatic interactions, such ion redistribution is highly dependent on the distribution of the electrostatic potential $\psi(r)$ in the space (for simplicity, the analysis will be restricted to only one coordinate, r position):

$$C_i = C_{0,i} \exp\left(\frac{-\psi(r) z_i e}{k_B T}\right) \quad (1)$$

where C_i and $C_{0,i}$ are the concentrations of i-compound at position r and in the bulk, respectively, k_B is the Boltzmann constant, T temperature, e is the electron charge, and z_i the ion valence.

At this point, it is necessary to introduce the Poisson–Boltzmann equation (for a complete derivation of this equation and their implications in ion transport through SSNs, we strongly recommend ref. 36 and 37):

$$\nabla^2\psi(r) = \frac{-e\sum_i C_i z_i}{\varepsilon\varepsilon_0} = \frac{-e}{\varepsilon\varepsilon_0} \times \sum_i C_{0,i} \exp\left(\frac{-\psi(r) z_i e}{k_B T}\right) z_i \quad (2)$$

where ε and ε_0 are the relative permittivities of the medium (usually water) and the vacuum, respectively. This equation describes the behavior of the electrostatic potential of the surface due to the presence of ions in solution.

Poisson–Boltzmann equation is a partial second order expression that can be analytically solved only for some geometries. For instance, assuming low-charged planar surfaces (Debye–Hückel approximation), it gives rise to the following expression:

$$\psi(r) = \psi_0 \exp(-\kappa r) \quad (3)$$

where ψ_0 is the electrostatic potential at the surface ($r = 0$) and κ is the Debye–Hückel parameter, a magnitude that depends on the variables related to the temperature and electrolyte solution:

$$\kappa = \frac{1}{\lambda_D} = \sqrt{\frac{2C_0 e^2}{\varepsilon\varepsilon_0 k_B T}} \quad (4)$$

κ can be also rewritten as the inverse of the Debye length (λ_D). The parameter λ_D is usually employed as the characteristic dimension of the EDL. Considering eqn (4), in aqueous solutions, λ_D takes values of a few nanometers depending on the electrolyte concentration and temperature. For instance, λ_D diminishes as the electrolyte concentration increases, *e.g.*, for a 1 : 1 salt at 25 °C, λ_D ranges from ~9.6 nm to ~0.3 nm if the electrolyte concentration in an aqueous solution is varied from 10^{-3} M to 1 M. From a phenomenological perspective, as the bulk concentration increases, there are more ions available at the proximity of the surface to screen the surface charges. This heightened screening, in turn, contributes to a more pronounced and rapid decay of ψ as the distance from the electrode increases.

Usually, it is easier to have an estimation of the surface charge density (σ) than ψ_0. Considering the electroneutrality principle and the Debye–Hückel approximation, it is possible to find an approximated expression for σ:

$$\sigma = \frac{\psi_0 \varepsilon\varepsilon_0}{\lambda_D} \quad (5)$$

Considering all this theoretical framework, it is possible to conclude that EDL, *i.e.* the portion of solution in the proximities (in the range of λ_D) to the surface, is characterized by an increase of the counterion (ions with a charge sign opposite to the surface charge) concentration and a depletion of the coion (ions with the same charge sign as the surface charge) concentration. Also, the degrees of ion enrichment and depletion are accentuated as σ increases. While these equations were derived in conditions that, in principle, are not compatible with the case of study of this review (channels with nanocurvature, not flat surface), the trends and qualitative behaviors observed in Debye–Hückel are still representatives in more complex systems.[19,38]

In the case of charged nanochannels, it is assumed that if the aperture radius is in the order of λ_D, the counterion enrichment due to the surface electrostatic potential promotes ion concentration polarization in the inner volume of the nanostructure. Thus, working with low/moderated electrolyte concentrations where the surface charges are not effectively screened enables the development of selective ion transport characteristics. On the contrary, in micrometric channels, the contribution of the EDL to the total volume of the channel is negligible and, in principle, it limits the possibility of obtaining ion selective behaviors. However, as will be seen below, this simplification can fail for the case of highly charged microchannels (see Dukhin length analysis).

Pioneer works by Renaud, Schoch, and coworkers demonstrated that the surface charge in silica nanoslits determines the ion transport through the nanostructure and, consequently, the iontronic output.[23,39,40] They demonstrated that the total conductance (G) in terms of the KCl concentration can be modeled as a superimposition of two different contributions: the bulk conductance given by the salt concentration and nanochannel dimensions (first term), and the ion excess conductance given by the effective σ (second term):

$$G = 1000(u_+ + u_-)C_0 N_A e\frac{wh}{L} + 2u_+\sigma\frac{w}{L} \qquad (6)$$

where u_+ and u_- are the mobilities of the cation and anion, respectively, w and h are the width and height of the nanoslits, respectively, N_A is the Avogadro number, and L the length. Therefore, they showed that, at low KCl concentrations between 10^{-6} M and 10^{-2} M (λ_D in the order of slit size), G remains almost constant, which is attributed to a surface charge-governed transport that generates an excess of mobile counterions inside of the nanoslit; *i.e.* second term $\gg$ first term. At high KCl concentrations ($>10^{-2}$ M), the first term is larger than the second term ($\lambda_D \ll$ slit size) and G follows a linear trend with the salt concentration, which indicates a bulk control of the iontronic response. Considering this, they demonstrated that, under appropriate conditions of ionic strength, the conductance of the nanostructure can be regulated by changing the surface charge density of the nanoslit. As will be addressed thorough this review, this conclusion is central for the actuation of a wide variety of nFET devices.

The ion transport characteristics of charged channels also depend on the nanofluidic device symmetry.[5,18,24] Symmetrical cylindrical channels usually exhibit a conductance value dependent on the surface charge but independent of the transmembrane voltage. Thus, the current–voltage curves (I–V) follow a linear trend whose slope (*i.e.* the conductance) is determined by the effective surface charge density, as schematized in Fig. 1(a). On the contrary, in asymmetric channels, the conductance depends on both the surface charge density and the transmembrane voltage. The I–V curves are characterized by a rectifying (ICR) behavior where the conductance at a given transmembrane voltage polarity is enhanced with respect to the opposite polarity (Fig. 1(b)).

Various theories attempt to elucidate the occurrence of ICR in the I–V curves of asymmetric channels. Among these theories, the most widely utilized is based on the accumulation–depletion of ions. This theory finds support in quantitative descriptions obtained through Poisson–Nernst–Planck (PNP) simulations conducted on geometrically asymmetric channels.[41,42] Fig. 2(a) presents the ion profiles inside a negatively charged conical nanochannel determined by PNP simulations. Within this theoretical framework, counterions are enriched in the tip region due to electrostatic interaction with the surface charges when they are driven from tip to base by applying a certain transmembrane voltage polarity. Simultaneously, coions are also enriched but in a lower degree to maintain the electroneutrality. This ion accumulation, in turn, generates enhancement in the current at a given transmembrane voltage polarity. For the case revisited in Fig. 2(a), such enhancement in the current is given at positive transmembrane voltages. It is worth mentioning that, as both kind of ions are enriched at this voltage polarity, the current presents a low selectivity, *i.e.* while the ratio of current (I) transported by cations ($|I_+/I|$) results higher to that transported by anions, both magnitudes are in the same order (Fig. 2(b)).

On the contrary, if transmembrane voltage polarity is now inverted, coions are forced to migrate from tip to base but their repulsive electrostatic interactions with the charged surface groups create a barrier to entry into the channel, leading to an ion depletion. Consequently, a low conductance state is established. For the case revisited in Fig. 2(a), such low conductance state is given at negative transmembrane voltages and, as shown Fig. 2(b), presents a high degree of ion selectivity. These trends have been schematized in Fig. 2(c) for the case of a negatively charged conical nanochannel. However, by using the same line of thinking, an analogous scheme can be obtained for positively charged conical channels.

Considering the origin of ICR, the efficiency of the rectification (*i.e.* the ratio between the currents at both transmembrane

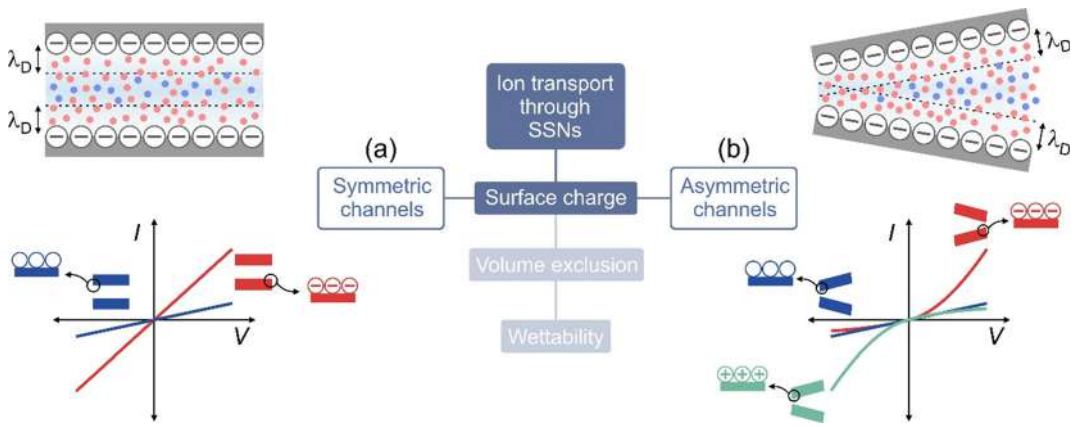

Fig. 1 Scheme illustrating the typical iontronic output (I–V curves) for (a) symmetric and (b) asymmetric channels. The scheme also indicates the dependence of the response on the surface charge density and polarity.

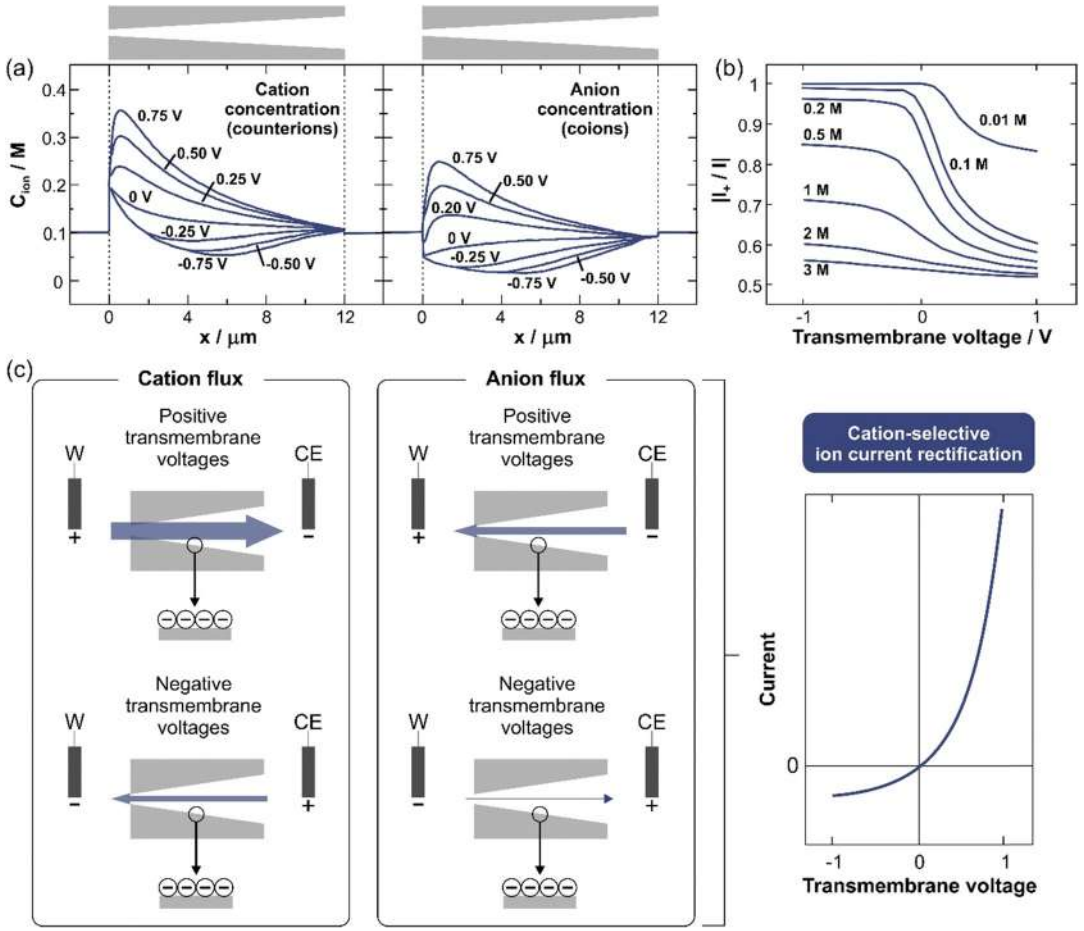

Fig. 2 (a) Ion concentration profiles at different channel regions (r). r = 0 μm and r = 12 μm correspond to the narrow (tip) and wide (base) apertures of the negatively charged conical nanochannel. (b) Ratio of the total current transported by cations at different transmembrane voltages. (c) Scheme that summarizes the cation and anion fluxes upon the different polarities of transmembrane voltage and the consequent current–voltage curve. Adapted with permissions from ref. 42, with permission from AIP Publishing, 2006.

voltage polarities) typically increases as the surface charge density increases (Fig. 1(b)).[43] However, as the ICR is closely related to the selectivity of the system, its efficiency is also very sensitive to other parameters such as the channel diameters and salt concentration. This fact makes difficult to find a general equation for the efficiency of the rectification in terms of the experimental variables and structural parameters of the channel. Although that, the trend between the rectification efficiency and the surface charge is widely employed for sensing purposes.[44]

Remarkably, ICR means a vectorial transport where the direction of the favored current depends on the surface charge polarity.[45–47] In other words, the transmembrane voltage polarity associated with higher conductance values is dictated by the type of net surface charge (Fig. 1(b)). As was exemplified in Fig. 2, if the ICR is dictated by a negatively charged surface, the behavior is referred to as cation-driven or cation-selective rectification due to the main contribution of cations to the current, and the high conductance branch is placed at positive transmembrane voltages (if working electrode is faced to the tip channel) (Fig. 1(b), red curve). However, if all the experimental conditions are maintained but, the polarity of the channel surface charge is inverted, the I–V curve exhibits the high conductance branch at negative transmembrane voltage and ICR is referred to as anion-driven or anion-selective rectification (Fig. 1(b), green curve).

Usually, it is assumed that a tip diameter in the nanometric range and moderated electrolyte concentration are required to obtain a λ_D/channel radius ratio suitable to evidence the ICR phenomenon. However, different reports have shown the possibility of fabricating highly-charged channels with micrometric apertures that still display ICR.[48,49] To explain that, it is necessary to introduce the Dukhin length (l_{Du}):

$$l_{Du} = \frac{|\sigma|}{eC_0} \quad (7)$$

This parameter represents the ratio between the surface and bulk conductivities and, in contrast to λ_D, its magnitude is sensitively affected by σ. A dimensionless Dukhin number (Du) can be introduced:

$$Du = \frac{2l_{Du}}{d} \quad (8)$$

where d is the channel diameter. A comprehensive analysis

from Bocquet's group based in theoretical calculations showed that when l_{Du} takes values in the order or higher than the channel radius (*i.e.* Du $>$ 1), the nanofluidic device can exhibit significant selectivity and rectification efficiencies. Therefore, this magnitude involves a more representative parameter of selectivity (and rectification) instead of the ratio λ_D/channel radius (further details are available in ref. 50) and explain the possibility to obtain ICR even in microchannels.

Volume exclusion

Frequently, the changes in the solution properties or the application of a certain stimulus can generate a rearrangement of the molecular systems grafted on the channel walls which gives rise to variations in the inner free volume and effective channel size.[25,51–53] In particular, the volume of the channel influences the number of ions to be transported and, therefore, a change in this parameter will trigger variations in the ion transport and the iontronic output (Fig. 3(a)). Consequently, a diminution in the inner free volume generates an increment in the membrane resistance.[23]

The great sensitivity of the iontronic signal to the changes in the channel-free volume has been also employed as a strategy for the development of nanofluidic biosensors.[53–56] In these cases, the recognition element is generally grafted onto the channel surface in such a way that the subsequent exposition to a bulky analyte (*e.g.*, proteins or viruses) produces appreciable changes in the inner volume and, consequently, in the iontronic signal.

It is worth mentioning that, for charged channels, a diminution in the channel volume might also generate an accentuation in the surface electrostatic potential inside of the channel due to the decrease in the effective channel size. Under this scenario, the accentuation of the influence of the charged surface groups can give rise to a more selective transport and, even, changes in the transport regimes.[57] This can be employed as a top-down approach to design permselective nanofluidic devices from micrometric channels. For instance, Pérez-Mitta *et al.* demonstrated that the immobilization of polydopamine onto the channel surface turns the transport from a non-selective ohmic behavior to a rectifying behavior due to the appreciable reduction of the channel tip size from the micrometric to the nanometric range.[58]

On the other hand, in certain devices where the channel dimensions are in the order of the hydrated ion radii, the steric effects take even more relevance. That is the case of the incipient field focused on the development of nanofluidic membranes modified with metal–organic frameworks. The integration of these materials, typically characterized by their microporosity (pore size $<$2 nm), triggers notable variations in the ion transport properties across the membrane.[59–61] For instance, several authors have shown the impossibility of certain ions being transported through the membrane due to the access impediment to the narrow ion paths provided by the MOF structure.[62] Furthermore, the combination of this strong reduction of the ion path size and surface charge might give rise to different iontronic output regimes such as ion saturation current.[57]

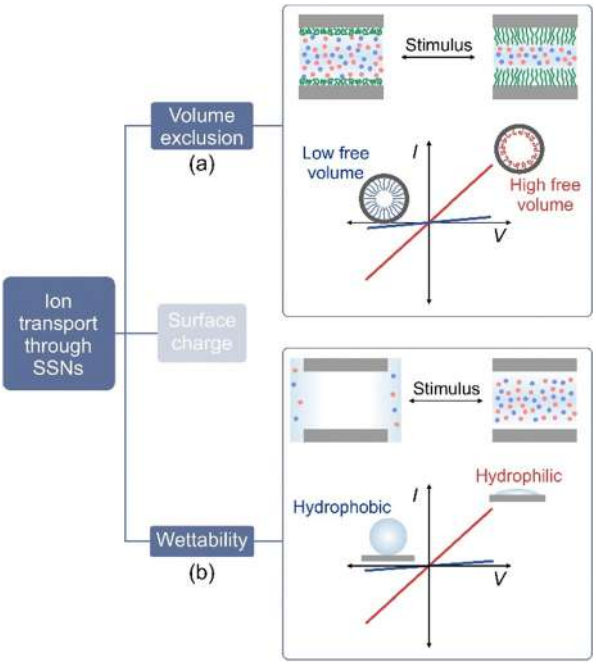

Fig. 3 Scheme illustrating the implications of the variations in the (a) free volume and (b) surface wettability of the channel over the *I*–*V* curves.

Wettability

Biological ion channels can regulate the ion flux by employing hydrophobic gating.[63,64] Similarly, ion transport in solid-state nanochannels can also be regulated by changes in the wettability properties of the surface. In these cases, the hydrophobic properties of the surface can act as an efficient permeation barrier due to the unfavorable interactions between the water and the surface that depletes water molecules (''dewetted'') in a given channel region (Fig. 3(b)). Under this condition, ion conduction is restricted due to the high energetic barrier.

It has been demonstrated that hydrophobicity changes promoted by the application of a certain stimulus can be employed as a very efficient ON/OFF switch.[65] For instance, Vlassiouk *et al.* introduced the creation of a light-controlled valve based on the modification of an alumina nanofluidic membrane with a photochromic spiropyran molecule.[66] Upon UV irradiation, the spyrocycle is transformed into its isomer. This change in the molecular system grafted on the channel walls triggers profound changes in the wettability properties of the membrane. Specifically, the surface switches from a non-wetted state (hydrophobic) to a fully wetted (hydrophilic) state which leads to an abrupt increment of two orders of magnitude in the ion conductance. More recently, Xie *et al.* showed a similar light-activated channel by modifying a polyimide nanochannel with an azobenzene derivate.[67] Interestingly, these authors demonstrated that the hydrophobic barrier can be broken by irradiating with appropriate light and increasing the transmembrane voltage magnitude. Similar behaviors have been reported in other systems.[68–72]

Nanofluidic field-effect transistors (nFETs) – definition and experimental setup

As was mentioned, the fundamental strategy to create stimulus-responsive systems is based on the immobilization of different responsive molecular systems onto the channel walls. In the case revisited here, we are interested in the application of a certain external voltage to promote changes in the physicochemical features of the channel walls and, concomitantly, in the ion transport and the iontronic output.

In analogy to electrolyte-gated field-effect transistors (FETs) where the application of a gate voltage modulates the electronic current between the drain and source electrodes (under a certain constant value of the voltage between drain and source), the main idea in nFET devices is that the external voltage modulates the ion current through the membrane (under a certain constant value of transmembrane voltage) (Fig. 4). From this analogy, voltage-gated nanofluidic devices are referred here to as nFETs whereas the external voltage is the so-called gate voltage (V_g). Noteworthy, signal carriers in nFETs are the ions which is an important difference compared to electrolyte-gated FETs where the signal is given by electrons and holes. For this reason, nFET devices are also referred to as ionic FETs in the bibliography.

In addition to the differences in the signal carriers, it is worth mentioning that the mechanisms that govern the response in each case are strongly different. As will be seen, in the case of nFETs, the signal modulation is given by the changes in the physicochemical properties of the channel (and membrane) surface promoted by the V_g action. On the other hand, in the case of electrolyte-gated FETs, a semiconducting material is connected between the source and drain electrodes and, connected to the gate electrode by an electrolyte solution.[73] The V_g application produces a drift of anions or cations towards the semiconductor channel that, in turn, enhance or deplete its charge carrier concentration. The V_g-controlled variations in the charge carrier concentration of the semiconducting material results in a modulation of its conductance.

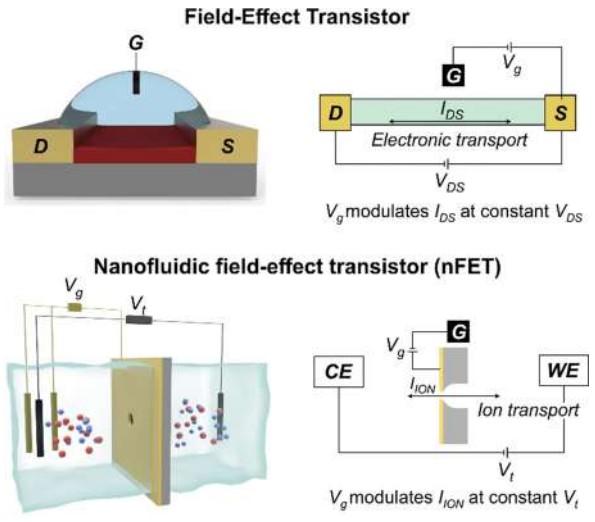

Fig. 4 Scheme illustrating the analogy between electrolyte-gated field-effect transistors and nanofluidic field-effect transistors (external voltage-controlled SSNs).

As expected, the observation of field effects on the nanofluidic transport requires the control of two different voltages, the transmembrane voltage (V_t) that forces the ion flow through the membrane and the external voltage (V_g) that acts as the stimulus. Experimentally, the membrane is placed between two reservoirs filled with electrolyte solutions, and a two or four-electrode arrangement is connected to a potentiostat to control V_t and, simultaneously, record the ion current (iontronic output). Moreover, nFETs also require the application of V_g (against a reference electrode) directly on the membrane surface. For this, it is necessary to deposit any conducting material (for example, a gold layer) onto the membrane surface. Such external voltages can be applied simultaneously or separately to the transmembrane voltage. In the first case, it is possible kinetics studies of the iontronic response towards the changes in V_g but, as a drawback, a bipotentiostatic mode is usually needed. In the second case, the membrane is exposed to a given V_g before the iontronic measurement.

Beyond the kinetic information, the main advantage of the bipotentiostat mode stems from the possibility of simultaneously obtaining two different signals. The electrochemical and iontronic currents that arise from the application of V_g and V_t, respectively. The former is mainly given by the electrochemical reactions or surface charge reorganization onto the membrane surface, while the latter is given by the ion transport across the channel and, consequently, it presents a main contribution to the surface effects of the channel walls. This fact not only allows a cross-verification of the actuation mechanism but also enables the creation of dual-signal devices for different purposes such as biosensing or fundamental studies.[74,75] Noteworthy, dual-signal offers more reliable sensing by minimizing the probability of false positives and, at the same time, makes possible a higher understanding of the sensing mechanism and its relation with the channel parameters.[76–78]

Fabrication and fundamental principles of nFETs

For most SSN nanofluidic devices the membranes employed have been polymeric track-etched membranes (polycarbonate -PC- and polyethylene terephthalate -PET-), aluminum oxide, and silicon-based channels. A short paragraph will be dedicated to briefly summarize the key aspects of each kind of SSN. Details on the different nanofabrication methods can be found in previous review articles and books.[18,19,25,36]

Silicon-based nanochannels and nanoslits can be created by different nanofabrication protocols.[31,79,80] One common method is the sacrificial layer method which includes optical

lithography and chemical treatments and results in silica nanoslits connected with two microchannels (the fluidic reservoirs).[79,81,82] Other nanofabrication methods have also employed sol–gel chemistry or e-beam lithography and etching treatments.[83,84] Multichannel aluminum and other metal oxide membranes with highly ordered symmetrical channels are typically obtained with different sizes and lengths by employing a two-step electrochemical anodization protocol.[25,85–87] Etched ion-track membranes have been synthesized in different materials including PC, PET, or polyimide by employing swift heavy ion irradiation and subsequent chemical etching.[34,88,89] By ion-track nanotechnology, remarkably, it is possible to independently control most of the relevant channel parameters such as density (channel number per area unit), geometry, and size.

One of the key aspects during the creation of the nFETs is the functionalization protocol that confers electrical responsiveness to the nanochannel surface. The nFET fabrication usually requires the integration of materials with appropriate electrical conductivity to the channel walls (or entrance) such as metals, metal oxides, or electroactive organic molecules. This fact has been mostly achieved by sputtering and electroless protocols. In the former, an inorganic layer (typically, gold, platinum, or indium tin oxide -ITO-) with a given thickness is deposited on the membrane surface. In these cases, the gating is mainly given by the outer membrane surface.[74] In the latter, the metal layer (typically Au) coats both the channel walls and the membrane surface. However, the integration of a homogeneous layer with small grain sizes and controlled thickness is not a trivial issue.[90] More details on the different nanofabrication methods can be found in ref. 18, 25 and 36.

To create nFETs, different building blocks and modification methods have been reported. Depending on the nature of the building blocks employed during the post-functionalization of the nanofluidic device surface, nFETs can be divided into three groups:

1. Inorganic nFETs: nanofluidic devices (inorganic or polymeric) post-functionalized with metals and inorganic oxides.

2. Inorganic/organic nFETs: nanofluidic devices (inorganic or polymeric) post-functionalized with both an inorganic coating (*e.g.* metals) and organic molecules (*e.g.* electroactive polymers).

3. Organic nFETs: nanofluidic devices (inorganic or polymeric) post-functionalized with only organic molecules (*e.g.* electroactive polymers).

In the following, some common aspects related to the creation and gating mechanisms of the different subclasses will be addressed.

Inorganic nFETs

In this category, the SSNs are directly modified with inorganic layers, typically gold or metal oxides, and different gate voltages are applied to the inorganic layer to control the surface charge excess which, in turn, modulates the ion current.[91] In the absence of applied V_g, ion transport is controlled by the native surface charge of the channel. However, the application of a specific V_g value can either increment (when V_g polarity aligns with the native charge), neutralize, or even reverse (when V_g polarity opposes the native charge) the polarity of the native surface charge.[32] The magnitude of the change is directly related to the magnitude of V_g. Pioneering works focused on the creation of external voltage-controlled actuators in different nanofluidic devices, including track-etched membranes,[92] silica-based channels,[82] and Si_3N_4 nanopores,[83] employed this approach.

Important advances in this kind of device were obtained by Charles Martin and coworkers in the late '90s.[92,93] In their studies, they demonstrated the possibility of creating nFETs by modifying multichannel track-etched PC membranes with cylindrical channels with a gold layer *via* electroless. In the presence of Cl^-, ion transport of metalized membranes was mainly governed by the surface charge provided by anion adsorption onto the gold layer. However, experiments conducted in KF salts or after the integration of a thiol onto the gold surface, where anion adsorption is prevented, displayed excellent ion transport modulation by V_g. Under those conditions, the authors demonstrated the possibility of varying the ion selectivity (given by the transference numbers) from almost ideal anion-selective to cation-selective by varying V_g from 0.4 V to −0.4 V. Remarkably, they also showed that selectivity can be enhanced by decreasing the effective channel size.

Further advances in inorganic nFETs based on track-etched membranes were demonstrated by Siwy's group. For instance, in 2009, Siwy and coworkers reported the creation of an nFET based on a track-etched PET membrane bearing a single conical channel with an insulated gold thin film as the gate electrode (Fig. 5(a)).[94] For this purpose, after the nanofabrication protocol, the track-etched membrane was modified on the tip side with a gold layer ($\sim$50 nm) and, subsequently, with a silicon dioxide layer ($\sim$50 nm) to isolate the gold. Before both gold and silicon dioxide deposition, a thin titanium oxide film ($<$15 nm) was integrated onto the membrane surface to improve the metal adhesion. In all the cases, oxide and metals were integrated by employing an electron beam evaporator. In the absence of V_g applied, the system exhibited a typical cation-driven rectification due to the presence of negatively charged groups on the silica surface. Counterintuitively, the application of $V_g < 0$ V produced the diminution of the rectification properties although an increment in the number of negatively charged sites was expected (Fig. 5(b)). The reason behind this behavior was attributed to an ion concentration polarization in the tip region promoting an ion depletion that caused an ion current saturation regime. The ion current saturation was more abrupt as V_g (and, therefore, surface charge) became more negative. On the contrary, the application of $V_g > 0$ V (and, $<$2 V) did not produce notable changes in the ion current due to the difficulty of overcoming the negative native charge of the silica layer.

Inorganic nFETs have been extensively studied by employing titanium and silicon-based nanofluidic channels.[31,79,83,84,95–98] For instance, pioneering works were reported by Karnik *et al.* employing arrays of silicon-based nanochannels.[79,98] In those works, they demonstrated the ability of nFETs to control not

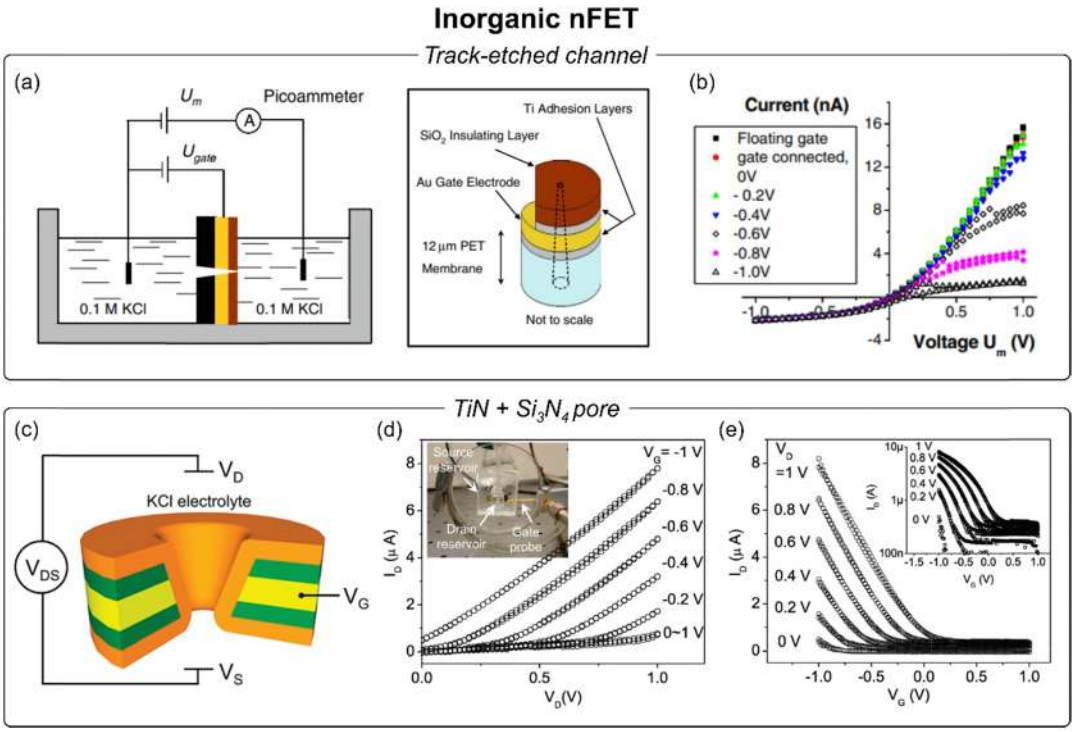

Fig. 5 Inorganic nFETs based on different kinds of nanofluidic devices. (a) Scheme illustrating the design of an inorganic nFET based on a track-etched conical nanochannel. (b) $I-V$ curves under different V_g applied. Reproduced with permissions from ref. 94. Copyright © 2008, The Author(s). (c) Scheme illustrating the design of an inorganic nFET based on a nitride-based nanopore. Yellow, green, and orange colors indicate TiN, Si_3N_4, and TiO_2 materials, respectively. (d) $I-V$ curves under different V_g applied. (e) Transmembrane ion current in terms of V_g for different V_t applied (in the graph V_D refers to V_t). Reproduced with permissions from ref. 83. Copyright © 2009, American Chemical Society.

only the ionic conductance but also the transport of fluorescent dyes, DNA chains, and labeled proteins by changing the V_g polarity and magnitude.

Nam *et al.* reported an nanopore array FET based on a TiN membrane sandwiched with Si_3N_4 dielectric films (Fig. 5(c)).[83] Such a nanofluidic device was firstly constructed by employing e-beam lithography and reactive ion etching and, then, modified with a TiO_2 *via* atomic layer deposition to control the final diameter in the sub-10 nm range. Employing the TiN film as a gate electrode, they showed the possibility of modulating the ion transport at low electrolyte concentrations ($<10^{-3}$ M) by modulating V_g. As shown in Fig. 5(d), the nFET displayed an increment of the ion current when V_g became more negative. Conversely, in the positive range of V_g, the ion current remained constant regardless of the magnitude of V_g (Fig. 5(e)). This trend, similar to the above-mentioned by Siwy and coworkers, was referred to as ''unipolar behavior''.

Due to the high charge density of silica, this kind of device usually presents a unipolar behavior (the system typically acts only as cation selective) because the high native surface charge cannot be overcome by the application of V_g.[83] To have complete control of the transport with the electrostatic field, a very low native or null surface charge is essential which can be easily achieved by employing post-functionalization methods.[98] For instance, Lee *et al.* demonstrated that this fact can be overcome by adding a layer of low surface charge such as Al_2O_3 and replacing the planar gate electrode (*i.e.* only in a given channel wall) with a gate electrode in the entire channel surface in such a way that changes in the V_g can be enough to exceed the native charge of the channel walls.[99] Notably, the sensitivity towards V_g increased, and the electrochemical nanoactuator displayed an ambipolar behavior with an extended operative range of electrolyte concentrations (<1 M KCl).

The first advances in this topic were obtained with inorganic nFETs. Remarkably, in the case of silicon-dioxide-based nanofluidic devices, it is possible to introduce different variations to the gate electrode position and geometry which provide different kinds of iontronic signals (see section ''Applications'').[82,99] Beyond the material of the nanofluidic device, the above-mentioned reports have shown the success of this strategy to remotely control the ion transport across the SSN in a rapid and non-invasive way by polarizing the gate electrode with relatively low voltage magnitudes ($|V_g| < 1$ V). One of the disadvantages of this approach seems to be the necessity to work with nanochannels with small diameters (<20 nm) which could be challenging from the nanofabrication perspective. Moreover, most of the results were obtained under low ionic strength (typically KCl concentrations <1 mM) providing low current magnitudes. As it was explained, the application of modification methods such as atomic layer or electroless depositions as top-down approaches and the design of all-around gate electrodes can be interesting strategies to overcome nanofabrication

challenges and ionic strength limitations, respectively. On the other hand, the high native charge of materials like silica or gold (in Cl^- bath) can lead to unipolar behavior or, even, to the impossibility of modulating the ion transport with V_g. For these cases, the modification of the surface with neutral or lowly charged materials (some thiols or Al_2O_3) can be a good alternative.

Inorganic/organic nFETs

Inorganic/organic nFETs include the modification of the nanofluidic device, typically a track-etched or alumina membrane, with a metal layer to provide conductive properties to the surface and, subsequently, the immobilization of an electroactive polymer layer, as shown in Fig. 6(a). For this purpose, electropolymerization has been the most employed method due to its advantages such as easy synthesis, good stability, and high thickness control. In particular, previous reports have shown that the increment of the polymer thickness leads to a diminution of the channel aperture.[100] Therefore, the electropolymerization protocol also provides the possibility to modulate the final nanochannel aperture. For its part, spin-coating represents a good option when the electropolymerization requires conditions difficult to make compatible with the nanofluidic membranes, for example, organic media.[101]

In contrast to inorganic nFETs, the gating mechanism in inorganic/organic nFETs is based on the redox transformation of the electroactive polymer and its concomitant variations in the physicochemical properties of the channel entrance surface. Thus, the application of different V_g controls the redox state of the electroactive polymer (and, therefore, its chemical structure) in the channel entrance. When the applied V_g is enough to promote the reduction or oxidation of the electroactive polymer, the variations in the surface charge, volume, or wettability of the electroactive polymer layer trigger modifications in the ion transport across the channel which, in turn, modify the iontronic signal.

In 2015, pioneering works by Azzaroni and coworkers reported the creation of this new generation of nFET based on the integration of a gold layer and polyaniline (PANI) onto the surface of a track-etched PC membrane bearing a single

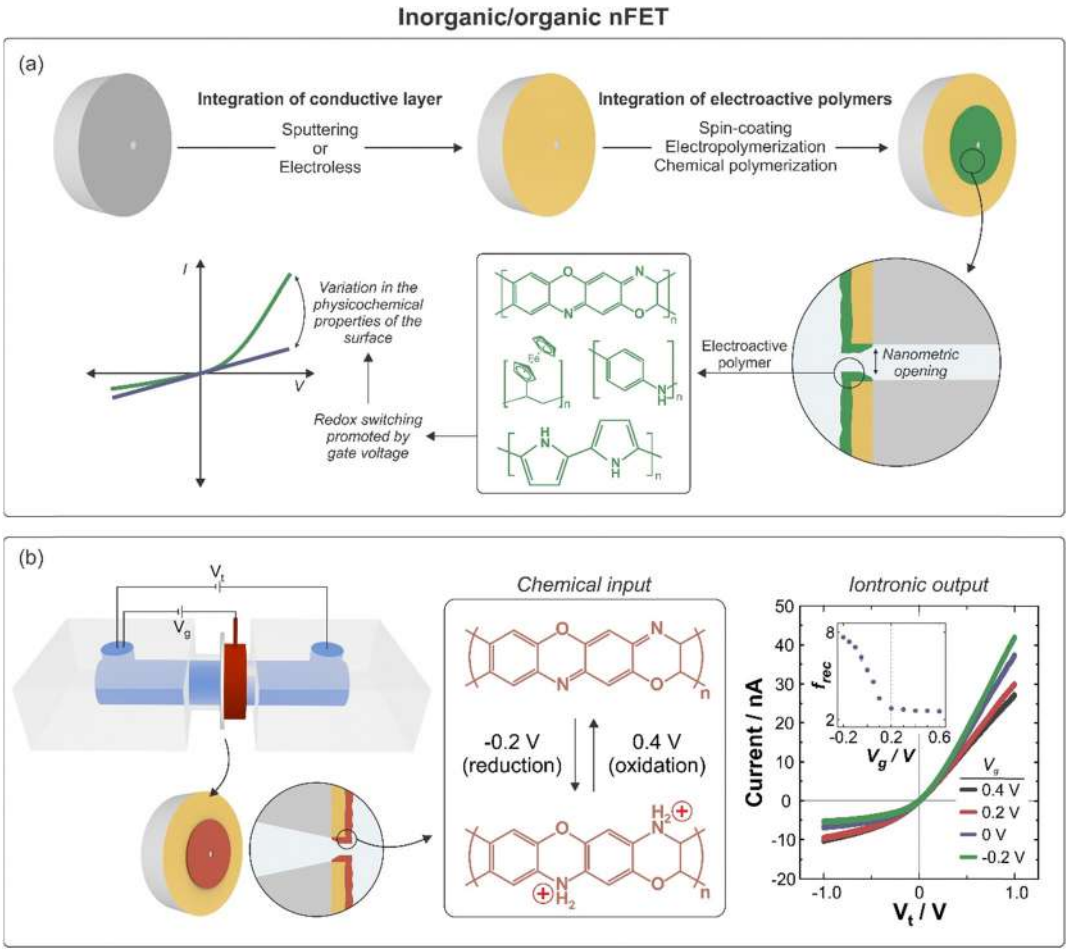

Fig. 6 (a) Scheme illustrating the general fabrication route and the relationship between the internal channel chemistry and the iontronic output in inorganic/organic nFETs. (b) Specific examples of the design illustrated in (a). The scheme shows the relationship between the construction, the chemical input, and the final iontronic output of an nFET based on metalized track-etched membranes modified with POAP. Adapted from ref. 103 with permission from the Royal Society of Chemistry.

conical channel.[100] PANI is a conducting polymer with three different redox states: leucoemeraldine (fully reduced), emeraldine (intermedium state), and pernigraniline (fully oxidized). A peculiarity of PANI is that its redox transformation is coupled to acid–base equilibria and, particularly, the number of positively charged sites in the layer increases as PANI is oxidized. Therefore, the modification of a single conical PC nanochannel with a gold layer *via* sputtering and, subsequently with a PANI film *via* electropolymerization allowed the electrochemical control of the surface charge density at the channel entrance. Thus, the application of $V_g > 0.2$ V caused the PANI oxidation from lecuoemeraldine to emeraldine which was transduced in an increment of the rectification properties (anion-driven rectification) due to the increase of the number of positively charged sites. In the last years, this concept was transferred to other electroactive polymers such as polypyrrole (PPy),[102] poly(vinylferrocene) (PVFc),[101] and poly-*o*-aminophenol (POAP).[103]

For instance, the integration of POAP onto the surface of a track-etched PET membrane with a single bullet-shaped channel demonstrated the possibility of modulating the ion transport from a low rectification to a high rectification state in 0.05 M $NaClO_4$ at pH 2 (Fig. 6(b)).[103] This fact was enabled by the increment of the charged state of POAP when the polymer is reduced upon the application of $V_g < 0.2$ V. Remarkably, this system displayed a very rapid (<2 seconds) and reversible (5 cycles) reconfiguration of the ion conductance to the different external voltages proving the potential of this technology to rapidly control the ion transport with a non-invasive stimulus.

The new generation of nFETs based on electroactive polymers presents several advantages. In particular, redox transformation of electroactive polymers is usually possible at low voltage magnitudes ($|V_g| < 1$ V) which offers the possibility to precisely modulate the ion transport by delivering low energy stimuli. Furthermore, the properties of electroactive polymers provide a reversible and rapid fine-tuning of the ion transport towards the different V_g. Also, the actuation of these devices has been demonstrated even in channels with tip diameters around 100 nm and with supporting electrolytes in concentrations of 0.1 M which results in higher currents and mass transport. On the other hand, the chemical properties of electroactive polymers make it possible to combine external voltage actuation with other functionalities such as pH, light, or chemical effectors responsiveness.[74,104–106] As a disadvantage, certain electroactive polymers require specific operative conditions for being reversible oxidized and reduced such as an acidic medium.[74]

Organic nFETs

One of the main requirements to create an nFET is the necessity to have a conducting surface to apply the different external voltages. In general, such condition is fulfilled by the integration of a metal or metal oxide layer with outstanding conductive properties, including gold, platinum, or ITO.[74,102,104] In 2018, Perez-Mitta *et al.* reported for the first time an all-plastic nFET, *i.e.* an nFET fabricated without adding any inorganic conductive layer onto the channel surface.[107] For this, the authors took advantage of the excellent conductive properties of the conducting polymer poly(3,4-ethylenedioxythiophene) (PEDOT) doped with tosylate (Fig. 7(a)). This fully organic nFET was based on a single bullet-shaped PET nanochannel modified with a layer of PEDOT of 60 nm of thickness deposited by spin-coating. Considering the net charge variation during PEDOT:tosylate redox transformation, the ion transport was modulated between cation-selective (fully reduced PEDOT, $V_g = -0.6$ V, OFF state at $V_t = 1$ V), non-selective (intermediate PEDOT state, $V_g = -0.2$ V) and anion-selective (fully oxidized PEDOT, $V_g = 0.8$ V, ON state at $V_t = 1$ V) (Fig. 7(b)). Consequently, the iontronic signal was switched between a cation-driven rectification, ohmic behavior, and anion-driven behavior, respectively (Fig. 7(c)).

The main advantage behind this strategy relies on its simplicity and cost-effectiveness. It allows the creation of a functional nFET with an external voltage-controlled ion transport in only one single step of postfunctionalization. Similar to inorganic/organic nFET, the actuation towards the different V_g is reversible and rapid, also, it can be achieved even in microchannels (tip diameter >100 nm) at moderated KCl concentrations (0.1 M). As a disadvantage, omitting the inorganic conductive layer is not feasible for every electroactive polymer. In this regard, PEDOT:tosylate exhibits exceptional

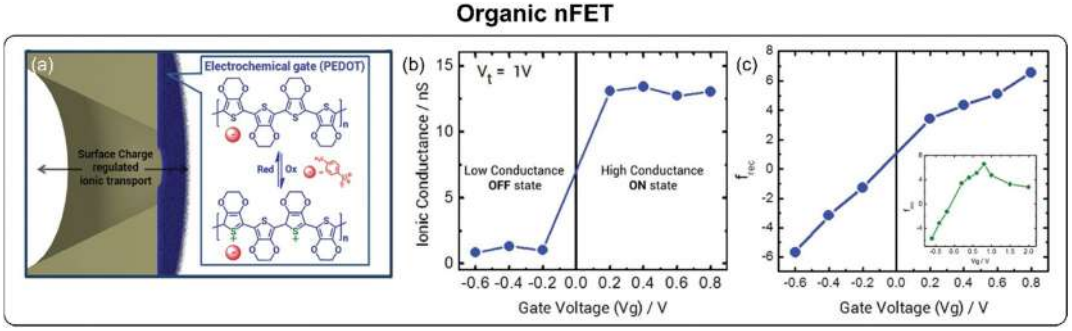

Fig. 7 Organic nFET. (a) Scheme of the organic nFET based on a single channel track-etched membrane modified with PEDOT:tosylate. Iontronic response in terms of the (b) ionic conductance and (c) rectification factor for the different applied external voltages. Reproduced with permissions from ref. 107. Copyright 2017, WILEY-VCH Verlag GmbH & Co. KGaA, Weinheim.

conductivity properties that make possible the electrochemical nanoactuation.

Features and applications

Generation and control of iontronic signals

Most of the proof of concepts behind the actuation of nFETs has been focused on the control/generation of iontronic signals and manipulation of matter. For instance, imparting asymmetry during the nanofabrication or modification enables the generation of nanofluidic devices with diode-like behavior with efficiency and magnitude that can be finely tuned by V_g. In these cases, the interplay between the structural or chemistry symmetry added to the modulation of charged groups given by the external voltage control has proven the possibility to alternate the signal between different iontronic states including, ohmic, cation-driven, and anion-driven rectification.

Recently, Fuest *et al.* demonstrated the possibility of modulating the current magnitude and direction by the gate potential.[95] They constructed an nFET device based on a borosilicate nanochannel with a gold gate electrode isolated from the solution by a polydimethylsiloxane layer (Fig. 8(a)). Remarkably, the ion current at fixed V_t = 3 V could be manipulated between three different states (forward, zero, and reverse currents) by changing V_g from +2 V to −2 V (Fig. 8(b)). The authors assumed that the V_g application alters the electric field in the proximity of the gate electrode and leads to the three current-state behavior. Such current modulation was maximum for 1 mM KCl (Fig. 8(c)).

In contrast to track-etched membranes, the use of silica channels provides the possibility to configure the position of the gate electrode which presents a crucial role in the final response.[108] Regarding this effect, Guan *et al.* introduced a voltage-gated silica channel with the ability to reconfigure the ion transport regime and the diode functions (direction and rectification efficiency) by adjusting the gate electrode position and V_g magnitude and polarity.[82] In this work, the authors demonstrated that it is possible to confer rectification properties to an array of symmetrical silica channels by asymmetrically positioning the gate electrode near one of the microfluidic reservoirs. Additionally, rectification direction can be modulated by varying the V_g polarity and, therefore, the type of excess surface charge. The magnitude of the rectification factor could be enhanced by increasing the $|V_g|$. Remarkably, they also showed the possibility of appreciably increasing the rectification efficiencies by including two gate electrodes to the nanofluidic device.

On the other hand, nFETs based on electroactive polymers have attracted special attention. In general, it is assumed that the selection of the electroactive polymer determines the actuation range because the gating mechanism relies on the physicochemical changes of the polymer during its redox transformation. For instance, the modification of only one side of nanofluidic devices with a metal layer and then, an electroactive polymer such as PVFc or PPy makes it possible to switch the iontronic output between an ohmic behavior to an anion-driven rectification upon the polymer oxidation.[101,102] This is because in both cases, PVFc and PPy, the polymer oxidation generates positively charged groups in the chain that modify the ion transport properties of the channel similarly. The presence of such charged groups added to the asymmetry imparted either during the modification or channel nanofabrication explains the diode-like behavior when V_g magnitude is enough to promote polymer oxidation.

Beyond the selection of the electroactive polymer nature, the iontronic signals can be effectively modulated with the geometry of the nanofluidic device. For instance, as it was mentioned above, the ion transport properties of conical channels modified with a gold layer and a PANI film can be alternated between rectification states of different efficiencies by controlling the V_g.[100] However, employing the same building blocks, Hu *et al.* introduced an nFET with the ability to switch the iontronic output from an ion current saturation regime to ohmic behavior by electrochemically changing the redox state of PANI.[109] For this, they reported the design of a PNP nanofluidic bipolar junction transistor by sandwiching a PANI film between two multichannel PET membranes bearing conical nanochannels. Therefore, if the V_g applied to the PANI layer was enough to promote the polymer oxidation ($V_g > 0$ V), the

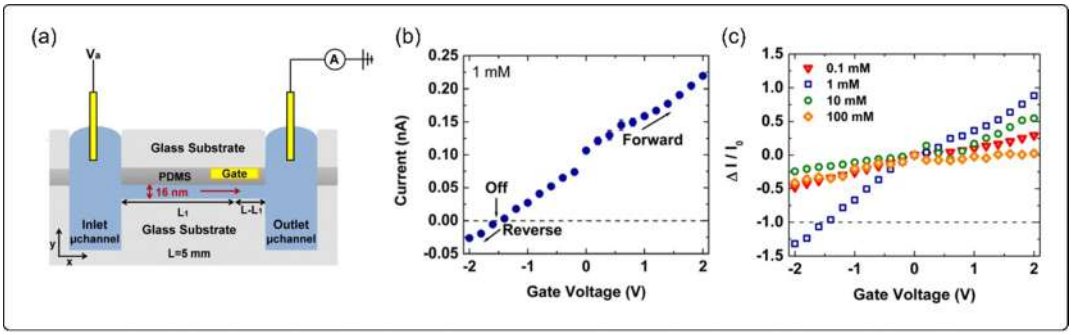

Fig. 8 (a) Scheme illustrating the design of an inorganic nFET based on a borosilicate nanochannel. (b) Transmembrane ion current in terms of V_g. (c) $I - I_0/I_0$ in terms of V_g for different electrolyte concentrations. I_0 refers to the current obtained at V_g = 0 V. In all the cases, V_t = 3 V. Reproduced with permissions from ref. 95. Copyright © 2015, American Chemical Society.

increment in the charged state of PANI generated a peculiar ion current saturation regime and, consequently, the *I–V* curve adopted a sigmoid shape (S-shape). Conversely, the reduction of the PANI triggered by $V_g < -0.5$ V led to an ohmic behavior due to the loss of charged sites in the polymer film.

So far, it has been demonstrated that the design of the nFET, including gate electrode position, electroactive polymer nature, and channel geometry, among others, enables the generation of different kinds of iontronic signals. However, another interesting aspect of inorganic/organic nFETs stems from the ability to confer other functionalities by exploiting the electrochemical richness of electroactive polymers which further expands its application field. For instance, Laucirica *et al.* demonstrated the possibility of finely tuning the iontronic signal, *i.e.* not only the rectification magnitude but also its direction, by harnessing the interplay between the redox transformation of POAP and its interaction with multivalent anions from the supporting electrolyte.[74] The nFET was created by modifying single-channel track-etched membranes bearing a single bullet-shaped nanochannel with a gold layer *via* sputtering and, subsequently, with a POAP film by electropolymerization (Fig. 9(a)). The use of KCl as a supporting electrolyte led to the expected anion-driven rectification due to the presence of positively charged amino groups of POAP (Fig. 9(b)). Such anion-driven rectification could be enhanced or turned off by applying a voltage of −0.2 V (total reduction) or 0.2 V (total oxidation). However, employing sulfate ions as the supporting electrolyte gave rise to a cation-driven rectification due to the local inversion of the charge promoted by the interaction of divalent anions with the amino groups from POAP (Fig. 9(c)). Under this condition, the cation-driven rectification could be enhanced or turned off by applying a V_g of 0.2 V (total oxidation) or 0.2 V (total reduction). The rectification efficiency (given by the rectification factor) could be precisely modulated by reducing and oxidizing the electroactive polymer in the range of $0.2\ \text{V} > V_g > -0.2\ \text{V}$. Therefore, by exploiting the combination of supporting electrolyte and gate voltage, the device could alternate between ohmic, anion-driven, and cation-driven rectifying regimes.

The interaction between the bath ions and the electroactive polymer can be also utilized to alter the gating mechanism. Exploiting this concept, Zhai and coworkers introduced the creation of an nFET by modifying an aluminum oxide multi-channel membrane with a gold layer and a PPy film doped with perfluorooctanesulfonate ($PFOS^-$).[110] Under a reduced state, PPy does not present charged groups, while its oxidation generates positively charged groups with a consequent entry of the bath's anions to the film.[102] For the case of experiments conducted in a tetraethylammonium-$PFOS^-$ salt, PPy oxidation (V_g = +1 V) drove the $PFOS^-$ ions into the film. Given the hydrophobic nature of the anion, the oxidation of PPy resulted in a superhydrophobic state where the ion transport is highly unfavoured. Conversely, the PPy reduction ($V_g = -0.6$ V) drove the anions out of the film resulting in a hydrophilic state that allowed a high flux of ions through the nanochannels. In conclusion, the precise and non-invasive electrochemical handle of the wettability properties allowed alternating between two current states: OFF (currents around 0.2 nA) at the superhydrophobic state, and ON (currents around 2 μA) at the hydrophilic state which represents a gating ratio around 1×10^4.

More recently, the modification of both apertures has been employed to generate devices with multi-state ion transport.[111,112] Wu *et al.* introduced a sandwiched nanofluidic

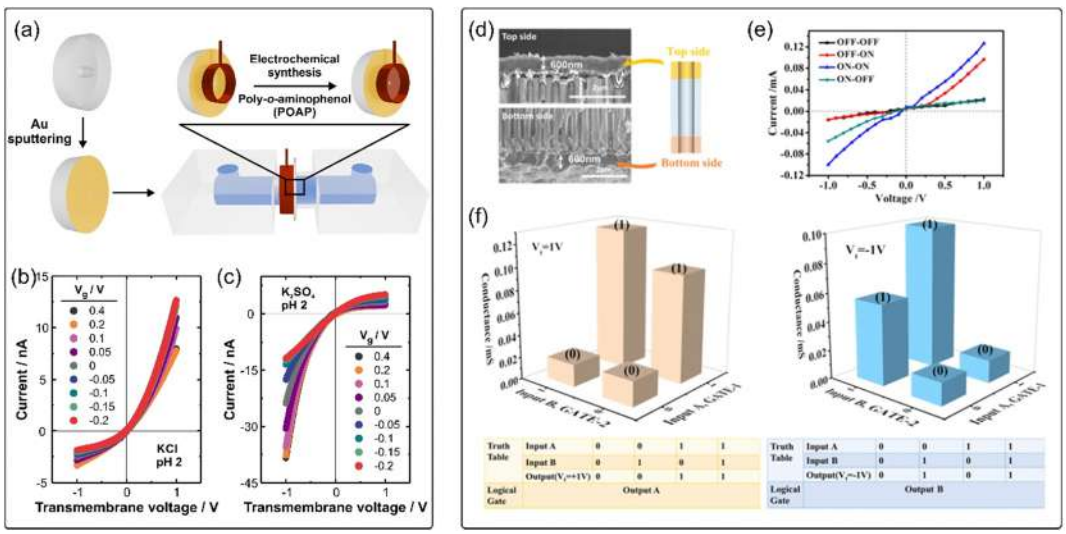

Fig. 9 (a) Scheme illustrating the construction of a POAP-based nFET. *I–V* curves at different V_g using (b) 0.1 M KCl and (c) 0.1 M K_2SO_4 as supporting electrolyte. Adapted from ref. 74 with permission from the Royal Society of Chemistry. (d) Cross-section SEM images of the AAO nanofluidic membrane modified at both sides with PPy. (e) *I–V* curves for the different redox states of PPy layers. ON and OFF refer to the oxidation state of the PPy layers. Thus, ON–ON and OFF–OFF indicate that both PPy layers were oxidized and reduced, respectively. (f) Conductance at ±1 V for the different combinations of redox states of the PPy layers. Inputs A and B refer to the V_g applied to each PPy layer. Reproduced with permissions from ref. 111. Copyright © 2021, American Chemical Society.

membrane based on the modification of both sides of a multichannel alumina foil with a gold layer and PPy film (Fig. 9(d)).[111] This double V_g-gated nanofluidic device allowed to oxidize or reduce the PPy layers at both membrane sides in an independent manner and, thus, to finely control the ion transport and iontronic response. For instance, when one of the PPy layers was oxidized (ON, V_g = +1 V) and the remaining one was reduced (OFF, V_g = −1 V), the device displayed ICR behavior as shown in Fig. 9(e). On the contrary, the *I–V* curves were linear for the symmetrical case, *i.e.* when both PPy layers were reduced (OFF–OFF) or oxidized (ON–ON). However, the ON–ON case exhibited maximum ion conductance while the OFF–OFF case showed a low ion transport magnitude. As a proof-of-concept, the device was employed to trigger different digital logical operations (Fig. 9(f)).

Filtration and drug delivery

Remarkably, the gating mechanism employed in these devices makes them very interesting for filtration and matter manipulation, since variations in the surface charge, inner volume, and wettability during the metal polarization or polymer redox transformation change their ion selectivity and transport capability. This applicability has been evidenced in both, inorganic nFETs and inorganic/organic nFETs.[113]

For instance, in 2005, Karnik *et al.* applied the variations in the surface charge of arrays of silica nanochannels triggered by V_g to control the transport of DNA through the nanofluidic device.[79] Then, they further expanded this concept and designed a silica-based inorganic nFET with two chromium gate electrodes.[98] In that work, they also modified the silica channel surface with the hydrophilic molecule 3-glycidoxypropyl trimethoxysilane to diminish the native surface charge and, thus, improve the electrostatic V_g control. By fluorescence measurements, they investigated how the V_g-induced surface charge affected the transport characteristics of the positively charged (labeled) avidin proteins. Specifically, the application of V_g = 1 V decreased the protein transport across the nFET due to the electrostatic repulsion of the proteins with the charged channel walls while, conversely, V_g = −1 V strongly incremented the avidin transport across the nanofluidic device due to the favorable interaction with the surface.

The pulsatile delivery of proteins has been also demonstrated in inorganic/organic nFETs. For instance, Jeon *et al.* introduced the creation of Au-metalized multichannel alumina membranes modified with PPy doped with the bulky anion dodecylbenzene sulfonate (DBS) to achieve this goal.[114] In this work, the pyrrole monomer was electropolymerized in the presence of DBS onto the Au-metalized membrane surface giving rise to a PPy film with DBS anions inside. When PPy is reduced (V_g = −1.1 V), the polymer chains become electrically neutral. This could generate either the DBS anions expulsion or cation entrance. Considering their size, DBS^- ions could not be expelled and, therefore, hydrated positive counterions ($Na^+ \cdot 3H_2O$) entered the PPy film, causing volume expansion of the electroactive polymer film. Instead, at the oxidation state

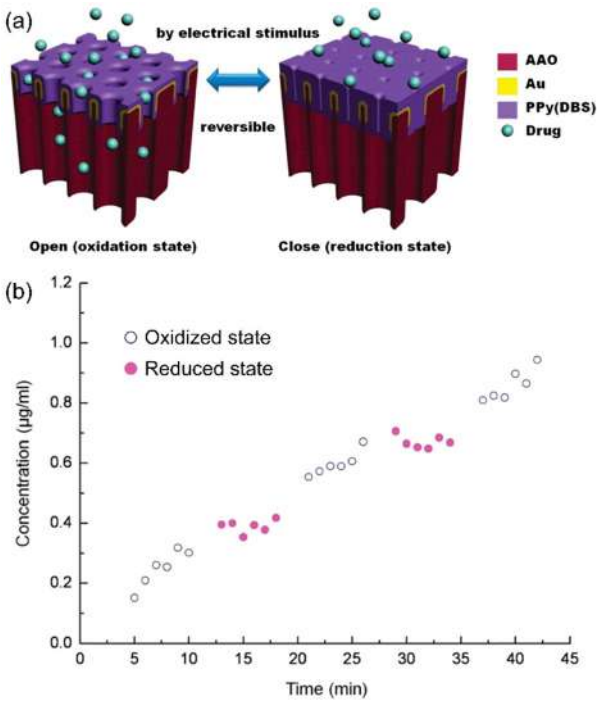

Fig. 10 (a) Gating mechanism of the PPy:DBS-based nFET. (b) Cumulative concentration fluorescein isothiocyanate-labeled bovine serum albumin in terms of time and under different V_g. Reproduced with permissions from ref. 114. Copyright © 2011, American Chemical Society.

(V_g = 0.2 V), PPy chains were positively charged, and hydrated positive counterions ($Na^+ \cdot 3H_2O$) were expelled from the film, resulting in volume shrinkage. The film volume expansion and shrinkage during reduction and oxidation, respectively, determined the effective aperture size and, consequently, the mass transport fluxes (Fig. 10(a)). Therefore, by exploiting the electrically modulated channel effective size, they demonstrated the pulsatile delivery of fluorescein isothiocyanate-labeled bovine serum albumin (Fig. 10(b)).

Similarly, the above-mentioned work from Zhai and coworkers applied PPy-based nFET with an electrically modulated wettability to control the release of penicillin and rhodamine B.[110] In this study, the external voltage modulated the wettability state of PPy by means of the entrance or exit of $PFOS^-$ which, in turn, promoted dramatic changes in the ion transport capability. In the superhydrophilic state, PPy film enabled the transport of the drugs while in the superhydrophobic state, such transport was prevented, giving a fine regulation of the drug release.

Dual-signal

Recently, dual-signal measurements have started to attract the attention of the scientific community in the field of SSNs. This kind of measurement consists of obtaining two different signals (simultaneously or not) with the same SSNs providing additional information for a given phenomenon. Some advantages of this dual-signal approach include cross-verifying the gating mechanism and extracting complementary information

to enhance process understanding.[77,115] In the case of devices applied for sensing purposes, dual-signal measurements could also offer the possibility to reduce false positives and increase detection selectivity.[55,76,78,116,117] Despite these advantages, the development of dual-signal devices remains to be explored.

Hao *et al.* developed a PANI-based nFET and monitored the changes in the redox switching due to the application of V_g *via* iontronic and spectroscopic measurements.[104] For this study, nanofluidic devices based in multichannel conical track-etched membranes were modified with a transparent ITO layer onto the tip side *via* sputtering and, subsequently, with a PANI film *via* electropolymerization. The ITO layer provides a good conductivity to establish different V_g and, at the same time, its transparent nature allows the spectroscopic measurement. PANI presents electrochromic properties, *i.e.* the redox switching promotes variations in the electronic structure of the polymer which, in turn, affects the light absorption properties. Therefore, the redox switching in PANI not only promotes variations in the charged state of the polymer but also in the film color. Taking advantage of this, the authors coupled *in situ* iontronic and spectrophotometric measurements. The oxidation of PANI at 1 mM KCl from leucoemeraldine to emeraldine state (V_g = 0.6 V) generated the appearance of rectification properties due to the increment in the PANI charged state and, at the same time, such redox switching increased the absorbance at 550 nm due to the PANI color change from yellow to green (Fig. 11(a) and (b)).

The bipotentiostatic arrangement makes possible to couple electrochemical and iontronic measurements. In the past, this strategy has been employed to correlate electrochemical information from the redox switching of the polymer with the iontronic information related to the ion transport across the membrane. For instance, Pérez-Mitta *et al.* employed chronoamperometry routines to determine the doping nature of the PEDOT:tosylate layer at different V_g and correlated them to the rectification factors obtained from the iontronic signals.[107] They found that the rectification factors and, consequently, the channel selectivities at different V_g were strongly related to the doping state of the PEDOT layer. Employing the same experimental setup, Laucirica *et al.* studied the gating performance of a POAP-based nFET at different pH values.[74] They found that the loss of sensitivity of the ion transport towards V_g variation at pH values >4 agreed with the decay of the oxidation peak current and its shift towards higher voltage values in the cyclic and square wave voltammetry (Fig. 11(c)–(f)). These results suggested that the loss of nFET functionality may be

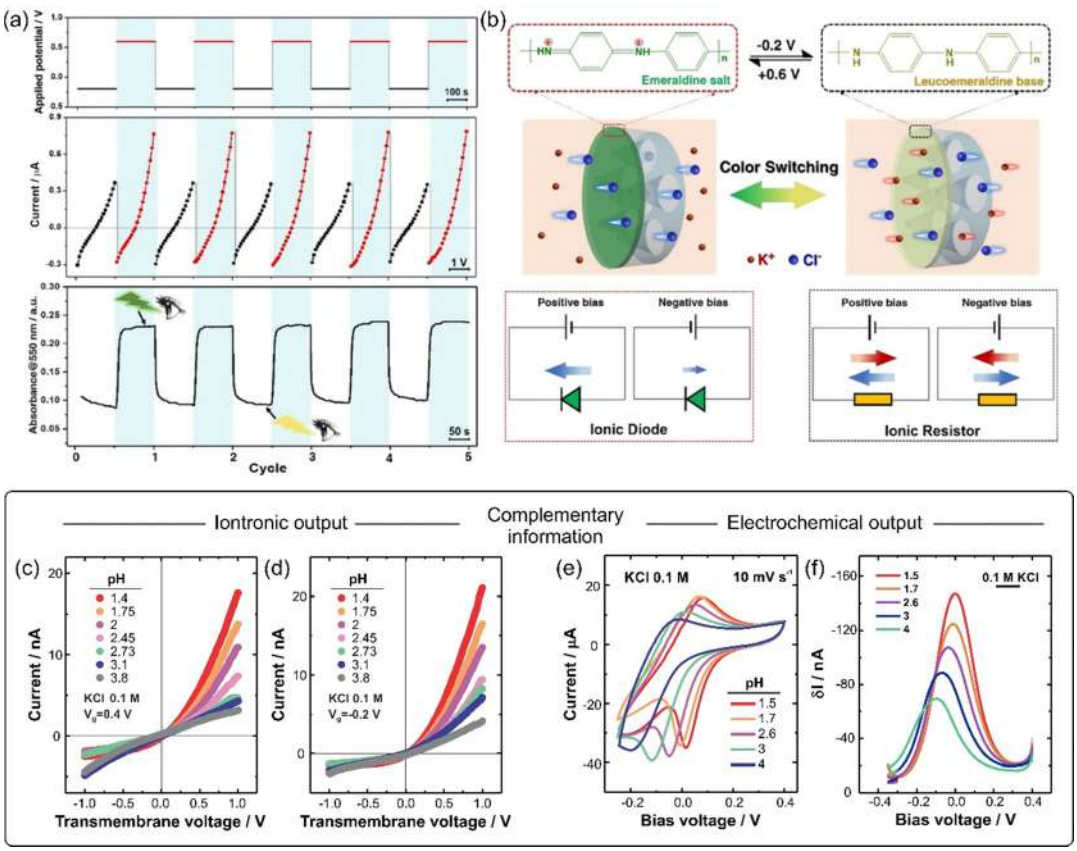

Fig. 11 (a) Plots of V_g *vs.* time, *I*–*V* curves, and absorbance at 550 nm *vs.* time (from top to bottom). (b) Scheme illustrating the correlation between the redox switching and the variations in the iontronic output and the color of the polymer. Reproduced with permissions from ref. 104. Copyright © 2020, American Chemical Society. *I*–*V* curves for a POAP-based nFET at (c) V_g = 0.4 V and (d) V_g = −0.2 V at different pH values (iontronic output). (e) Cyclic and (f) square wave voltammetry obtained for the POAP-based nFET at different pH conditions (electrochemical output). Reproduced from ref. 74 with permission from the Royal Society of Chemistry.

associated with the decrease of redox activity of POAP at pH values >4.

(Bio)sensing purposes

Beyond the above-mentioned applications related to iontronic manipulation and nanoelectronics, nFET has shown interesting results for (bio)sensing purposes. In particular, the modulation of the charged state of the surface with the gate electrode has been shown to produce appreciable changes in the translocation speed of biomolecules through the nanofluidic device which represents an advantage of this technology.[32,118–121] Taking into account the effects in the biomolecule translocations, most of the examples of nFET-based sensors were conducted with solid-state nanopores and used resistive-pulse as the sensing approach; however, this concept has been also demonstrated in SSNs.[122] In this sensing strategy, a fixed transmembrane voltage is typically applied and the analyte flows through the nanopore. If the analyte size is comparable to the pore aperture size, it produces considerable variations in the ion resistance which are evidenced as single-molecule pulse events in current–time curves. Such pulse events are characterized by the appearance frequency, dwell time, and current magnitude, among other parameters. The use of the nanopore surface as a gate electrode can trigger sensitive variations in the frequency, amplitude, and duration of such pulse events.

Korchev and coworkers designed an nFET based on a double-barrel quartz nanopipette for biosensing purposes (Fig. 12(a)).[123] For this purpose, one of the barrels was filled with pyrolytic carbon to act as the gate electrode and, the other barrel represented the nanopore. Then, the carbon electrode was coated with PPy by electropolymerization. Remarkably, the nFET-based sensor enabled the modulation of several parameters very relevant for the sensing of a DNA chain, including dwell times, event frequency, and signal-to-noise ratio by applying different V_g (Fig. 12(b)). For instance, the application of a V_g = 0.4 V triggered an increment of the event frequency, dwell time, and signal-to-noise ratio (Fig. 12(c)). This was attributed to the PPy oxidation and the consequent generation of positively charged groups that could electrostatically interact with the negatively charged DNA molecules producing the analyte enrichment in the aperture proximity and, also, the slowing down of the translocation event. In contrast, event frequency and dwell time dramatically decreased if $V_g = -0.4$ V. Additionally, the authors demonstrated that, taking advantage of the chemistry of electroactive polymers, they could use the PPy film not only as the gate electrode but also as a functional layer where a recognition element could be attached. For this study, they embedded insulin into the PPy film by electropolymerizing pyrrole in the presence of insulin and, demonstrated the ability of the PPy-based nFET to efficiently detect insulin antibodies. This concept has also proven to be advantageous for other analytes.[124]

Recently, Edel and coworkers further expanded the potentialities of nFET-based sensors. They developed a nFET based on a double-barrel quartz nanopipette with one of the barrels filled with pyrolytic carbon and, then, coated with a gold layer.[75] This work not only demonstrates the ability to module the sensing

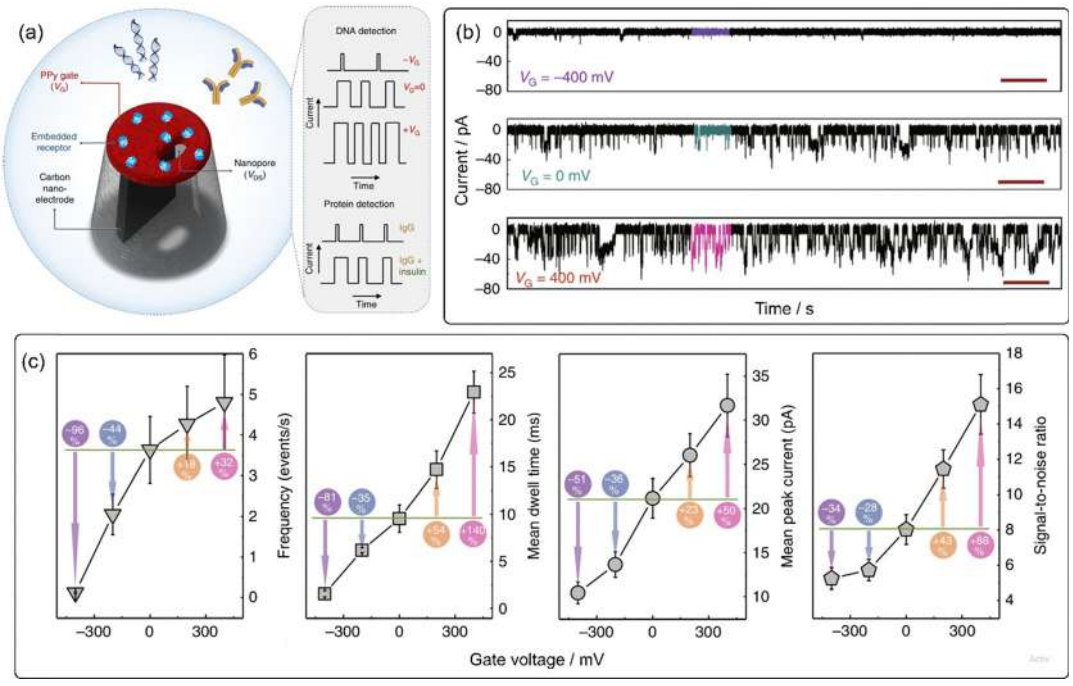

Fig. 12 (a) Scheme of the nFET-based sensor. The scheme also shows the implication of V_g and embedding the receptor (insulin) in the current–time curves for DNA sensing and antibody sensing, respectively. (b) Translocation recordings (current *vs.* time curves) for 300 pM of a double-strand DNA (3 kbp) in 0.1 M KCl at different V_g (V_t fixed at 0.7 V). The scale bar corresponds to 5 seconds. (c) Effect of V_g in the main analytical parameters of DNA sensing. Adapted with permissions from ref. 123. Copyright © 2017, The Author(s).

signal by applying different V_g to the gold layer but also introduces the possibility of conducting dual-signal sensing experiments. The device effectively sensed DNA chains through both the iontronic output generated during DNA translocation and the electrochemical signal obtained from the gate electrode. This study highlights the high potential of nFET-based sensors to enhance nanofluidic technologies' sensing performance while utilizing the advantages of dual-signal sensing.

Challenges and perspectives of the field

The field of nFETs holds great promise, but it also faces several challenges and presents intriguing perspectives for future research and practical applications.

One of the challenges is the creation of nFETs operative in a wide range of external conditions (pH, electrolyte concentration, *etc.*) Indeed, several inorganic/organic nFETs based on electroactive polymers have demonstrated outstanding performance, but only under specific conditions (*e.g.*, acidic pH), which limits their usability.[74,100,103] Similarly, the operational conditions in inorganic nFETs are often limited to low to moderate electrolyte concentrations. Another challenge is the demonstration of the long-term stability of the devices. The nFETs offer remarkable functionality in terms of ion transport modulation, however, questions persist about how these systems will perform over extended periods of operation.[114] Will the redox transformations that underpin their operation degrade the polymer film over time? How will the metal coatings on the nanochannel membranes fare under continuous operation? To fully exploit the potential of nFETs, it will be important to carry out such assessments to ensure their reliability in practical applications.

In the case of inorganic nFETs, the metal layer, typically based on gold, provides several opportunities for further functionalization, either through electrosynthesis or thiol chemistry, to render responsiveness to, *e.g.*, pH, analyte, or temperature, thereby further expanding the applicability of nFET devices. Similarly, the post-functionalization of electroactive polymers or their combination with other dopant materials or supporting electrolytes could also open new avenues in the development of functional organic or inorganic/organic nFETs.[74,110]

The emergence of all-plastic nFETs here referred to as organic nFETs, presents an exciting prospect for the field. Unlike traditional nFETs, these devices eliminate the need for metal deposition on the channel surface. This characteristic not only simplifies the nanofabrication but also potentially reduces costs significantly. However, despite their promise, research into all-plastic nFETs remains relatively scarce. To unlock their full potential, more studies are required to explore their fabrication processes, understand their behavior, and assess their suitability for various applications.

While nFETs have showcased their ability to control and generate iontronic signals effectively and manipulate (bio)molecule transport at the nanoscale, their concrete applications have not been extensively explored. These devices possess the potential to revolutionize fields such as nanoelectronics, logical devices, and lab-on-a-chip systems. Moreover, nFETs could open doors to developing dual-signal devices, allowing for a broader range of functionalities, for example, for sensing purposes. Consequently, nFETs offer a wide range of opportunities to bridge the gap between theoretical potential and practical implementation. Recent investigations have made remarkable progress in this direction, yielding promising results and intensifying interest in this class of devices.[104,111,123,124]

Conclusions

This review highlights the recent developments of nanofluidic field-effect transistors (nFETs) which regulate the ion and mass transport by applying an external voltage, which opened up a wide array of applications in drug delivery, biosensing, and nanoelectronics. The examples presented in the review illustrate the critical role that the internal architecture and chemistry of SSNs play, emphasizing the significance of material selection and surface modification in constructing functional nanofluidic devices.

The integration of stimulus-responsive properties into abiotic SSNs, inspired by the adaptability of biological ion channels, represents a promising avenue for creating advanced nanofluidic devices. This review has highlighted the essential requirement for external stimuli to induce changes in the physicochemical features of the channel surfaces, encompassing surface charge, wettability, and inner volume alterations.

Drawing an analogy with electrolyte-gated field-effect transistors (FETs), nanofluidic field-effect transistors (nFETs) operate on the principle that external voltage (gate voltage, V_g) modulates ion current through the membrane, similar to how gate voltage modulates electronic current in FETs. Notably, in nFETs, ions serve as signal carriers, distinguishing them from electronic FETs. The necessity to control two distinct voltages, transmembrane voltage (V_t) and external voltage (V_g), is crucial for observing field effects on nanofluidic transport.

The creation and modification of nFETs involve various materials, with polymeric track-etched membranes, aluminum oxide, and silicon-based channels being commonly employed. Key aspects of each SSN type were briefly summarized, emphasizing their distinct nanofabrication methods and applications. The integration of materials with suitable electrical conductivity onto the channel walls, achieved through sputtering or electroless protocols, is crucial for conferring electrical responsiveness to the nanofluidic surface.

Categorizing nFETs into inorganic, inorganic/organic, and organic types based on the nature of building blocks used for post-functionalization, the review touched upon common aspects related to their creation and gating mechanisms. Each subclass involves different combinations of inorganic coatings, organic molecules, and electroactive polymers to achieve

stimulus responsiveness. This classification provides a framework for understanding the diverse strategies employed in the development of nFETs.

The dual-signal capability of nFETs, obtained through the bipotentiostat mode, allows simultaneous recording of electrochemical and iontronic currents. This feature provides cross-verification of the actuation mechanism and opens avenues for creating dual-signal devices with applications in biosensing and fundamental studies. The bipotentiostat mode enhances sensing reliability by minimizing false positives and contributes to a deeper understanding of sensing mechanisms in relation to channel parameters.

As the field progresses, addressing challenges related to material selection, fabrication methods, and integration of responsive building blocks onto SSNs will be crucial. The insights provided in this review serve as a foundation for future research directions, encouraging interdisciplinary collaboration to unlock the full potential of external voltage-controlled SSNs in diverse technological applications. The evolving landscape of ion transport in nanofluidic devices promises exciting possibilities, and this review aims to contribute to the continued advancement of this rapidly evolving field.

Conflicts of interest

There are no conflicts to declare.

Acknowledgements

G. L. acknowledges the scholarship from CONICET. W. A. M., and O. A. acknowledge the financial support from Universidad Nacional de La Plata (PPID-X867), CONICET (PIP-0370), and ANPCyT (PICT-2017-1523 and PICT-2016-1680). M. E. T.-M. and V. C. acknowledge financial support by the initiative and networking fund of the Helmholtz Association of German Research Centers under the CORAERO Project (Grant KA1-Co-06).

References

1 B. Hille, *Ion Channels of Excitable Membranes*, Sinauer Associates Inc., Sunderland, 3rd edn, 2001.
2 D. A. Doyle, J. M. Cabral, R. A. Pfuetzner, A. Kuo, J. M. Gulbis, S. L. Cohen, B. T. Chait and R. MacKinnon, The Structure of the Potassium Channel: Molecular Basis of K^+ Conduction and Selectivity, *Science*, 1998, **280**, 69–77.
3 J. Zheng and M. C. Trudeau, *Handbook of ion channels*, CRC Press, Taylor & Francis Group, 2015.
4 E. Gouaux and R. MacKinnon, Principles of Selective Ion Transport in Channels and Pumps, *Science*, 2005, **310**, 1461–1465.
5 G. Pérez-Mitta, A. G. Albesa, C. Trautmann, M. E. Toimil-Molares and O. Azzaroni, Bioinspired integrated nanosystems based on solid-state nanopores: ''iontronic'' transduction of biological, chemical and physical stimuli, *Chem. Sci.*, 2017, **8**, 890–913.
6 X. Kan, C. Wu, L. Wen and L. Jiang, Biomimetic Nanochannels: From Fabrication Principles to Theoretical Insights, *Small Methods*, 2022, **6**, 2101255.
7 X. Hou, W. Guo and L. Jiang, Biomimetic Smart Nanopores and Nanochannels, *Chem. Soc. Rev.*, 2011, **40**, 2385–2401.
8 H. Chun and T. D. Chung, Iontronics, *Annu. Rev. Anal. Chem.*, 2015, **8**, 441–462.
9 G. Pérez-Mitta, A. G. Albesa, W. Knoll, C. Trautmann, M. E. Toimil-Molares and O. Azzaroni, Host–guest supramolecular chemistry in solid-state nanopores: potassium-driven modulation of ionic transport in nanofluidic diodes, *Nanoscale*, 2015, **7**, 15594–15598.
10 G. Pérez-Mitta, L. Burr, J. S. Tuninetti, C. Trautmann, M. E. Toimil-Molares and O. Azzaroni, Noncovalent functionalization of solid-state nanopores *via* self-assembly of amphipols, *Nanoscale*, 2016, **8**, 1470–1478.
11 V. M. Cayón, G. Laucirica, Y. Toum Terrones, M. L. Cortez, G. Pérez-Mitta, J. Shen, C. Hess, M. E. Toimil-Molares, C. Trautmann, W. A. Marmisollé and O. Azzaroni, Borate-driven ionic rectifiers based on sugar-bearing single nanochannels, *Nanoscale*, 2021, **13**, 11232–11241.
12 G. Pérez-Mitta, A. G. Albesa, M. E. Toimil-Molares, C. Trautmann and O. Azzaroni, The Influence of Divalent Anions on the Rectification Properties of Nanofluidic Diodes: Insights from Experiments and Theoretical Simulations, *ChemPhysChem*, 2016, **17**, 2718–2725.
13 G. Laucirica, Y. Toum Terrones, V. M. Cayón, M. L. Cortez, M. E. Toimil-Molares, C. Trautmann, W. A. Marmisollé and O. Azzaroni, High-sensitivity detection of dopamine by biomimetic nanofluidic diodes derivatized with poly(3-aminobenzylamine), *Nanoscale*, 2020, **12**, 18390–18399.
14 Y. Toum Terrones, G. Laucirica, V. M. Cayón, G. E. Fenoy, M. L. Cortez, M. E. Toimil-Molares, C. Trautmann, W. A. Mamisollé and O. Azzaroni, Highly sensitive acetylcholine biosensing *via* chemical amplification of enzymatic processes in nanochannels, *Chem. Commun.*, 2022, **58**, 10166–10169.
15 G. Pérez-Mitta, A. S. Peinetti, M. L. Cortez, M. E. Toimil-Molares, C. Trautmann and O. Azzaroni, Highly Sensitive Biosensing with Solid-State Nanopores Displaying Enzymatically Reconfigurable Rectification Properties, *Nano Lett.*, 2018, **18**, 3303–3310.
16 M. Ali, B. Yameen, R. Neumann, W. Ensinger, W. Knoll and O. Azzaroni, Biosensing and supramolecular bioconjugation in single conical polymer nanochannels. Facile incorporation of biorecognition elements into nanoconfined geometries, *J. Am. Chem. Soc.*, 2008, **130**, 16351–16357.
17 M. Tagliazucchi and I. Szleifer, Transport mechanisms in nanopores and nanochannels: Can we mimic nature?, *Mater. Today*, 2015, **18**, 131–142.
18 G. Pérez-Mitta, M. E. Toimil-Molares, C. Trautmann, W. A. Marmisollé and O. Azzaroni, Molecular Design of Solid-State Nanopores: Fundamental Concepts and Applications, *Adv. Mater.*, 2019, **31**, 1901483.
19 G. Laucirica, M. E. Toimil-Molares, C. Trautmann, W. Marmisollé and O. Azzaroni, Nanofluidic osmotic power

generators – advanced nanoporous membranes and nanochannels for blue energy harvesting, *Chem. Sci.*, 2021, **12**, 12874–12910.
20 G. Laucirica, A. G. Albesa, M. E. Toimil-Molares, C. Trautmann, W. A. Marmisollé and O. Azzaroni, Shape Matters: Enhanced Osmotic Energy Harvesting in Bullet-shaped Nanochannels, *Nano Energy*, 2020, **71**, 104612.
21 Y. Huang, W. Zhang, F. Xia and L. Jiang, Solid-State Nanochannel-Based Sensing Systems: Development, Challenges, and Opportunities, *Langmuir*, 2022, **38**, 2415–2422.
22 X. Hou and L. Jiang, Learning from Nature: Building Bio-Inspired Smart Nanochannels, *ACS Nano*, 2009, **3**, 3339–3342.
23 R. B. Schoch, J. Han and P. Renaud, Transport phenomena in nanofluidics, *Rev. Mod. Phys.*, 2008, **80**, 839–883.
24 Z. S. Siwy, Ion-current rectification in nanopores and nanotubes with broken symmetry, *Adv. Funct. Mater.*, 2006, **16**, 735–746.
25 G. Laucirica, Y. Toum Terrones, V. Cayón, M. L. Cortez, M. E. Toimil-Molares, C. Trautmann, W. Marmisollé and O. Azzaroni, Biomimetic solid-state nanochannels for chemical and biological sensing applications, *TrAC, Trends Anal. Chem.*, 2021, **144**, 116425.
26 Y. Toum Terrones, V. M. Cayón, G. Laucirica, M. L. Cortez, M. E. Toimil-Molares, C. Trautmann, W. A. Marmisollé and O. Azzaroni, in *Miniaturized Biosensing Devices*, Springer Nature Singapore, Singapore, 2022, pp. 57–81.
27 L. J. Cheng and L. J. Guo, Nanofluidic diodes, *Chem. Soc. Rev.*, 2010, **39**, 923–938.
28 Z. Siwy, P. Apel, D. Dobrev, R. Neumann, R. Spohr, C. Trautmann and K. Voss, Ion transport through asymmetric nanopores prepared by ion track etching, *NNucl. Instrum. Methods Phys. Res., Sect. B*, 2003, **208**, 143–148.
29 P. Y. Apel, I. V. Blonskaya, O. L. Orelovitch, P. Ramirez and B. A. Sartowska, Effect of nanopore geometry on ion current rectification, *Nanotechnology*, 2011, **22**, 175302.
30 C. Wei, A. J. Bard and S. W. Feldberg, Current Rectification at Quartz Nanopipet Electrodes, *Anal. Chem.*, 1997, **69**, 4627–4633.
31 S. Prakash and A. T. Conlisk, Field effect nanofluidics, *Lab Chip*, 2016, **16**, 3855–3865.
32 N. Hu, Y. Ai and S. Qian, Field effect control of electrokinetic transport in micro/nanofluidics, *Sens. Actuators, B*, 2012, **161**, 1150–1167.
33 T. Ma, J. M. Janot and S. Balme, Track-Etched Nanopore/Membrane: From Fundamental to Applications, *Small Methods*, 2020, **4**, 1–36.
34 M. E. Toimil-Molares, Characterization and properties of micro- and nanowires of controlled size, composition, and geometry fabricated by electrodeposition and ion-track technology, *Beilstein J. Nanotechnol.*, 2012, **3**, 860–883.
35 C. Duan, W. Wang and Q. Xie, Review article: Fabrication of nanofluidic devices, *Biomicrofluidics*, 2013, **7**, 26501.
36 M. Tagliazucchi and I. Szleifer, *Chemically Modified Nanopores and Nanochannels*, Elsevier Inc., 1st edn, 2016.
37 H.-J. Butt, K. Graf and M. Kappl, *Physics and Chemistry of Interfaces*, 2003.
38 P. C. Hiemenz and R. Rajagopalan, *Principles of Colloid and Surface Chemistry*, Marcel Dekker, 3rd edn, 1997.
39 R. B. Schoch and P. Renaud, Ion transport through nanoslits dominated by the effective surface charge, *Appl. Phys. Lett.*, 2005, **86**, 253111.
40 R. B. Schoch, H. van Lintel and P. Renaud, Effect of the surface charge on ion transport through nanoslits, *Phys. Fluids*, 2005, **17**, 100604.
41 J. Wang, M. Zhang, J. Zhai and L. Jiang, Theoretical simulation of the ion current rectification (ICR) in nanopores based on the Poisson–Nernst–Planck (PNP) model, *Phys. Chem. Chem. Phys.*, 2014, **16**, 23–32.
42 J. Cervera, B. Schiedt, R. Neumann, S. Mafé and P. Ramírez, Ionic conduction, rectification, and selectivity in single conical nanopores, *J. Chem. Phys.*, 2006, **124**, 104706.
43 G. Pérez-Mitta, A. Albesa, F. M. Gilles, M. E. Toimil-Molares, C. Trautmann and O. Azzaroni, Noncovalent Approach toward the Construction of Nanofluidic Diodes with pH-Reversible Rectifying Properties: Insights from Theory and Experiment, *J. Phys. Chem. C*, 2017, **121**, 9070–9076.
44 S. Zhang, W. Chen, L. Song, X. Wang, W. Sun, P. Song, G. Ashraf, B. Liu and Y.-D. Zhao, Recent advances in ionic current rectification based nanopore sensing: a mini-review, *Sens. Actuators, Rev.*, 2021, **3**, 100042.
45 G. Pérez-Mitta, W. A. Marmisollé, A. G. Albesa, M. E. Toimil-Molares, C. Trautmann and O. Azzaroni, Phosphate-Responsive Biomimetic Nanofluidic Diodes Regulated by Polyamine-Phosphate Interactions: Insights into Their Functional Behavior from Theory and Experiment, *Small*, 2018, **14**, 1702131.
46 G. Laucirica, G. Pérez-Mitta, M. E. Toimil-Molares, C. Trautmann, W. A. Marmisollé and O. Azzaroni, Amine-Phosphate Specific Interactions within Nanochannels: Binding Behavior and Nanoconfinement Effects, *J. Phys. Chem. C*, 2019, **123**, 28997–29007.
47 B. Yameen, M. Ali, R. Neumann, W. Ensinger, W. Knoll and O. Azzaroni, Single Conical Nanopores Displaying pH-Tunable Rectifying Characteristics. Manipulating Ionic Transport With Zwitterionic Polymer Brushes, *J. Am. Chem. Soc.*, 2009, **131**, 2070–2071.
48 M. Gao, P. Tsai, Y. Su, P. Peng and L. Yeh, Single Mesopores with High Surface Charges as Ultrahigh Performance Osmotic Power Generators, *Small*, 2020, **16**, 2006013.
49 C. Lin, L. Yeh and Z. S. Siwy, Voltage-Induced Modulation of Ionic Concentrations and Ion Current Rectification in Mesopores with Highly Charged Pore Walls, *J. Phys. Chem. Lett.*, 2018, **9**, 393–398.
50 A. R. Poggioli, A. Siria and L. Bocquet, Beyond the Tradeoff: Dynamic Selectivity in Ionic Transport and Current Rectification, *J. Phys. Chem. B*, 2019, **123**, 1171–1185.
51 B. Yameen, M. Ali, R. Neumann, W. Ensinger, W. Knoll and O. Azzaroni, Ionic transport through single solid-state

nanopores controlled with thermally nanoactuated macromolecular gates, *Small*, 2009, **5**, 1287–1291.

52 W. Guo, H. Xia, F. Xia, X. Hou, L. Cao, L. Wang, J. Xue, G. Zhang, Y. Song, D. Zhu, Y. Wang and L. Jiang, Current rectification in temperature-responsive single nanopores, *ChemPhysChem*, 2010, **11**, 859–864.

53 J. Guo, L. Yang, H. Xu, C. Zhao, Z. Dai, Z. Gao and Y. Song, Biomineralization-Driven Ion Gate in TiO_2 Nanochannel Arrays for Cell H_2S Sensing, *Anal. Chem.*, 2019, **91**, 13746–13751.

54 A. S. Peinetti, R. J. Lake, W. Cong, L. Cooper, Y. Wu, Y. Ma, G. T. Pawel, M. E. Toimil-Molares, C. Trautmann, L. Rong, B. Mariñas, O. Azzaroni and Y. Lu, Direct detection of human adenovirus or SARS-CoV-2 with ability to inform infectivity using DNA aptamer-nanopore sensors, *Sci. Adv.*, 2021, **7**, eabh2848.

55 R. Zhang, X. Chen, Z. Sun, S. Chen, J. Gao, Y. Sun and H. Li, Switchable Nanochannel Biosensor for H_2S Detection Based on an Azide Reduction Reaction Controlled BSA Aggregation, *Anal. Chem.*, 2019, **91**, 6149–6154.

56 N. Liu, R. Hou, P. Gao, X. Lou and F. Xia, Sensitive Zn^{2+} sensor based on biofunctionalized nanopores *via* combination of DNAzyme and DNA supersandwich structures, *Analyst*, 2016, **141**, 3626–3629.

57 G. Laucirica, J. A. Allegretto, M. F. Wagner, M. E. Toimil-Molares, C. Trautmann, M. Rafti, W. Marmisollé and O. Azzaroni, Switchable Ion Current Saturation Regimes Enabled via Heterostructured Nanofluidic Devices Based on Metal–Organic Frameworks, *Adv. Mater.*, 2022, 2207339.

58 G. Pérez-Mitta, J. S. Tuninetti, W. Knoll, C. Trautmann, M. E. Toimil-Molares and O. Azzaroni, Polydopamine Meets Solid-State Nanopores: A Bioinspired Integrative Surface Chemistry Approach to Tailor the Functional Properties of Nanofluidic Diodes, *J. Am. Chem. Soc.*, 2015, **137**, 6011–6017.

59 J. Lu, H. Xu, H. Yu, X. Hu, J. Xia, Y. Zhu, F. Wang, H.-A. Wu, L. Jiang and H. Wang, Ultrafast rectifying counter-directional transport of proton and metal ions in metal-organic framework–based nanochannels, *Sci. Adv.*, 2022, **8**, eabl5070.

60 H. Zhang, J. Hou, Y. Hu, P. Wang, R. Ou, L. Jiang, J. Z. Liu, B. D. Freeman, A. J. Hill and H. Wang, Ultrafast selective transport of alkali metal ions in metal organic frameworks with subnanometer pores, *Sci. Adv.*, 2018, **4**, eaaq0066.

61 X. Li, H. Zhang, P. Wang, J. Hou, J. Lu, C. D. Easton, X. Zhang, M. R. Hill, A. W. Thornton, J. Z. Liu, B. D. Freeman, A. J. Hill, L. Jiang and H. Wang, Fast and selective fluoride ion conduction in sub-1-nanometer metal-organic framework channels, *Nat. Commun.*, 2019, **10**, 2490.

62 J. Lu, H. Zhang, J. Hou, X. Li, X. Hu, Y. Hu, C. D. Easton, Q. Li, C. Sun, A. W. Thornton, M. R. Hill, X. Zhang, G. Jiang, J. Z. Liu, A. J. Hill, B. D. Freeman, L. Jiang and H. Wang, Efficient metal ion sieving in rectifying subnanochannels enabled by metal–organic frameworks, *Nat. Mater.*, 2020, **19**, 767–774.

63 P. Aryal, M. S. P. Sansom and S. J. Tucker, Hydrophobic Gating in Ion Channels, *J. Mol. Biol.*, 2015, **427**, 121–130.

64 O. Beckstein and M. S. P. Sansom, Liquid–vapor oscillations of water in hydrophobic nanopores, *Proc. Natl. Acad. Sci. U. S. A.*, 2003, **100**, 7063–7068.

65 X. Zhang, H. Liu and L. Jiang, Wettability and Applications of Nanochannels, *Adv. Mater.*, 2019, **31**, 1804508.

66 I. Vlassiouk, C.-D. Park, S. A. Vail, D. Gust and S. Smirnov, Control of Nanopore Wetting by a Photochromic Spiropyran: A Light-Controlled Valve and Electrical Switch, *Nano Lett.*, 2006, **6**, 1013–1017.

67 G. Xie, P. Li, Z. Zhao, Z. Zhu, X. Y. Kong, Z. Zhang, K. Xiao, L. Wen and L. Jiang, Light- and Electric-Field-Controlled Wetting Behavior in Nanochannels for Regulating Nanoconfined Mass Transport, *J. Am. Chem. Soc.*, 2018, **140**, 4552–4559.

68 M. R. Powell, L. Cleary, M. Davenport, K. J. Shea and Z. S. Siwy, Electric-field-induced wetting and dewetting in single hydrophobic nanopores, *Nat. Nanotechnol.*, 2011, **6**, 798–802.

69 Y. Fang, W. Xu, L. Yang, H. Qu, W. Wang, S. Zhang and H. Li, Electricity-Wettability Controlled Fast Transmission of Dopamine in Nanochannels, *Small*, 2023, **19**, 2205488.

70 J. Dzubiella and J.-P. Hansen, Electric-field-controlled water and ion permeation of a hydrophobic nanopore, *J. Chem. Phys.*, 2005, **122**, 234706.

71 S. Vaitheeswaran, J. C. Rasaiah and G. Hummer, Electric field and temperature effects on water in the narrow nonpolar pores of carbon nanotubes, *J. Chem. Phys.*, 2004, **121**, 7955–7965.

72 J. Dzubiella, R. J. Allen and J.-P. Hansen, Electric field-controlled water permeation coupled to ion transport through a nanopore, *J. Chem. Phys.*, 2004, **120**, 5001–5004.

73 F. Torricelli, D. Z. Adrahtas, Z. Bao, M. Berggren, F. Biscarini, A. Bonfiglio, C. A. Bortolotti, C. D. Frisbie, E. Macchia, G. G. Malliaras, I. McCulloch, M. Moser, T.-Q. Nguyen, R. M. Owens, A. Salleo, A. Spanu and L. Torsi, Electrolyte-gated transistors for enhanced performance bioelectronics, *Nat. Rev. Methods Prim.*, 2021, **1**, 66.

74 G. Laucirica, Y. Toum Terrones, M. F. P. Wagner, V. M. Cayón, M. L. Cortez, M. E. Toimil-Molares, C. Trautmann, W. Marmisollé and O. Azzaroni, Electrochemically addressed FET-like nanofluidic channels with dynamic ion-transport regimes, *Nanoscale*, 2023, **15**, 1782–1793.

75 L. Xue, P. Cadinu, B. Paulose Nadappuram, M. Kang, Y. Ma, Y. Korchev, A. P. Ivanov and J. B. Edel, Gated Single-Molecule Transport in Double-Barreled Nanopores, *ACS Appl. Mater. Interfaces*, 2018, **10**, 38621–38629.

76 X. Lou, Y. Song, R. Liu, Y. Cheng, J. Dai, Q. Chen, P. Gao, Z. Zhao and F. Xia, Enzyme and AIEgens Modulated Solid-State Nanochannels: In Situ and Noninvasive Monitoring of H_2O_2 Released from Living Cells, *Small Methods*, 2020, **4**, 1900432.

77 X. Li, T. Zhai, P. Gao, H. Cheng, R. Hou, X. Lou and F. Xia, Role of outer surface probes for regulating ion gating of nanochannels, *Nat. Commun.*, 2018, **9**, 647.

78 J.-J. Hu, W. Jiang, Q. Chen, R. Liu, X. Lou and F. Xia, Solid-State Nanochannel with Multiple Signal Outputs for Furin Detection Based on the Biocompatible Condensation Reaction, *Anal. Chem.*, 2021, **93**, 14036–14041.
79 R. Karnik, R. Fan, M. Yue, D. Li, P. Yang and A. Majumdar, Electrostatic Control of Ions and Molecules in Nanofluidic Transistors, *Nano Lett.*, 2005, **5**, 943–948.
80 M. Pinti, T. Kambham, B. Wang and S. Prakash, Fabrication of Centimeter Long, Ultra-Low Aspect Ratio Nanochannel Networks in Borosilicate Glass Substrates, *J. Nanotechnol. Eng. Med.*, 2013, **4**, 020905.
81 R. Karnik, K. Castelino, R. Fan, P. Yang and A. Majumdar, Effects of Biological Reactions and Modifications on Conductance of Nanofluidic Channels, *Nano Lett.*, 2005, **5**, 1638–1642.
82 W. Guan, R. Fan and M. A. Reed, Field-effect reconfigurable nanofluidic ionic diodes, *Nat. Commun.*, 2011, **2**, 506.
83 S. W. Nam, M. J. Rooks, K. B. Kim and S. M. Rossnagel, Ionic field effect transistors with sub-10 nm multiple nanopores, *Nano Lett.*, 2009, **9**, 2044–2048.
84 R. Fan, S. Huh, R. Yan, J. Arnold and P. Yang, Gated proton transport in aligned mesoporous silica films, *Nat. Mater.*, 2008, **7**, 303–307.
85 A. Ruiz-Clavijo, O. Caballero-Calero and M. Martín-González, Revisiting anodic alumina templates: from fabrication to applications, *Nanoscale*, 2021, **13**, 2227–2265.
86 J. H. Yuan, F. Y. He, D. C. Sun and X. H. Xia, A Simple Method for Preparation of Through-Hole Porous Anodic Alumina Membrane, *Chem. Mater.*, 2004, **16**, 1841–1844.
87 G. D. Sulka, J. Kapusta-Kołodziej, A. Brzózka and M. Jaskuła, Fabrication of nanoporous TiO_2 by electrochemical anodization, *Electrochim. Acta*, 2010, **55**, 4359–4367.
88 P. Y. Apel and D. Fink, in *Transport Processes in Ion-Irradiated Polymers*, ed. D. Fink, Springer-Verlag Berlin Heidelberg, 2004, pp. 147–202.
89 R. Spohr, *Ion Tracks and Microtechnology*, Vieweg + Teubner Verlag, Wiesbaden, 1st edn, 1990.
90 F. Muench, U. Kunz, C. Neetzel, S. Lauterbach, H.-J. Kleebe and W. Ensinger, 4-(Dimethylamino)pyridine as a Powerful Auxiliary Reagent in the Electroless Synthesis of Gold Nanotubes, *Langmuir*, 2011, **27**, 430–435.
91 H. Daiguji, P. Yang and A. Majumdar, Ion Transport in Nanofluidic Channels, *Nano Lett.*, 2004, **4**, 137–142.
92 M. Nishizawa, V. P. Menon and C. R. Martin, Metal Nanotubule Membranes with Electrochemically Switchable Ion-Transport Selectivity, *Science*, 1995, **268**, 700–702.
93 S. B. Lee and C. R. Martin, Controlling the Transport Properties of Gold Nanotubule Membranes Using Chemisorbed Thiols, *Chem. Mater.*, 2001, **13**, 3236–3244.
94 E. B. Kalman, O. Sudre, I. Vlassiouk and Z. S. Siwy, Control of ionic transport through gated single conical nanopores, *Anal. Bioanal. Chem.*, 2009, **394**, 413–419.
95 M. Fuest, C. Boone, K. K. Rangharajan, A. T. Conlisk and S. Prakash, A Three-State Nanofluidic Field Effect Switch, *Nano Lett.*, 2015, **15**, 2365–2371.
96 M. Fuest, K. K. Rangharajan, C. Boone, A. T. Conlisk and S. Prakash, Cation Dependent Surface Charge Regulation in Gated Nanofluidic Devices, *Anal. Chem.*, 2017, **89**, 1593–1601.
97 R. Fan, M. Yue, R. Karnik, A. Majumdar and P. Yang, Polarity switching and transient responses in single nanotube nanofluidic transistors, *Phys. Rev. Lett.*, 2005, **95**, 086607.
98 R. Karnik, K. Castelino and A. Majumdar, Field-effect control of protein transport in a nanofluidic transistor circuit, *Appl. Phys. Lett.*, 2006, **88**, 128–131.
99 S.-H. Lee, H. Lee, T. Jin, S. Park, B. J. Yoon, G. Y. Sung, K.-B. Kim and S. J. Kim, Sub-10 nm transparent all-around-gated ambipolar ionic field effect transistor, *Nanoscale*, 2015, **7**, 936–946.
100 G. Pérez-Mitta, W. A. Marmisollé, C. Trautmann, M. E. Toimil-Molares and O. Azzaroni, Nanofluidic Diodes with Dynamic Rectification Properties Stemming from Reversible Electrochemical Conversions in Conducting Polymers, *J. Am. Chem. Soc.*, 2015, **137**, 15382–15385.
101 G. Laucirica, W. A. Marmisollé, M. E. Toimil-Molares, C. Trautmann and O. Azzaroni, Redox-Driven Reversible Gating of Solid-State Nanochannels, *ACS Appl. Mater. Interfaces*, 2019, **11**, 30001–30009.
102 Q. Zhang, Z. Zhang, H. Zhou, Z. Xie, L. Wen, Z. Liu, J. Zhai and X. Diao, Redox switch of ionic transport in conductive polypyrrole-engineered unipolar nanofluidic diodes, *Nano Res.*, 2017, **10**, 3715–3725.
103 G. Laucirica, V. M. Cayón, Y. Toum Terrones, M. L. Cortez, M. E. Toimil-Molares, C. Trautmann, W. A. Marmisollé and O. Azzaroni, Electrochemically addressable nanofluidic devices based on PET nanochannels modified with electropolymerized poly-*o*-aminophenol films, *Nanoscale*, 2020, **12**, 6002–6011.
104 Z. Hao, T. Zhou, T. Xiao, H. Gong, Q. Zhang, H. Wang and J. Zhai, Electrochromic Nanochannels for Visual Nanofluidic Manipulation in Integrated Ionic Circuits, *ACS Appl. Mater. Interfaces*, 2020, **12**, 57314–57321.
105 Q. Zhang, Z. Liu, K. Wang and J. Zhai, Organic/Inorganic Hybrid Nanochannels Based on Polypyrrole-Embedded Alumina Nanopore Arrays: pH- and Light-Modulated Ion Transport, *Adv. Funct. Mater.*, 2015, **25**, 2091–2098.
106 G. Pérez-Mitta, W. A. Marmisolle, L. Burr, M. E. Toimil-Molares, C. Trautmann and O. Azzaroni, Proton-Gated Rectification Regimes in Nanofluidic Diodes Switched by Chemical Effectors, *Small*, 2018, **14**, 1703144.
107 G. Pérez-Mitta, W. A. Marmisollé, C. Trautmann, M. E. Toimil-Molares and O. Azzaroni, An All-Plastic Field-Effect Nanofluidic Diode Gated by a Conducting Polymer Layer, *Adv. Mater.*, 2017, **29**, 1700972.
108 Y. Ai, J. Liu, B. Zhang and S. Qian, Ionic current rectification in a conical nanofluidic field effect transistor, *Sens. Actuators, B*, 2011, **157**, 742–751.
109 Y.-L. Hu, Y. Hua, Z.-Q. Pan, J.-H. Qian, X.-Y. Yu, N. Bao, X.-L. Huo, Z.-Q. Wu and X.-H. Xia, PNP Nanofluidic Transistor with Actively Tunable Current Response and Ionic Signal Amplification, *Nano Lett.*, 2022, **22**, 3678–3684.

110 Q. Zhang, J. Kang, Z. Xie, X. Diao, Z. Liu and J. Zhai, Highly Efficient Gating of Electrically Actuated Nanochannels for Pulsatile Drug Delivery Stemming from a Reversible Wettability Switch, *Adv. Mater.*, 2017, **30**, 1703323.

111 M.-Y. Wu, Z.-Q. Li, G.-L. Zhu, Z.-Q. Wu, X.-L. Ding, L.-Q. Huang, R.-J. Mo and X.-H. Xia, Electrochemically Switchable Double-Gate Nanofluidic Logic Device as Biomimetic Ion Pumps, *ACS Appl. Mater. Interfaces*, 2021, **13**, 32479–32485.

112 R. Wu, J. Hao, Y. Cui, J. Zhou, D. Zhao, S. Zhang, J. Wang, Y. Zhou and L. Jiang, Multi-Control of Ion Transport in a Field-Effect Iontronic Device based on Sandwich-Structured Nanochannels, *Adv. Funct. Mater.*, 2023, **33**, 2208095.

113 S. Kim, E. I. Ozalp, M. Darwish and J. A. Weldon, Electrically gated nanoporous membranes for smart molecular flow control, *Nanoscale*, 2018, **10**, 20740–20747.

114 G. Jeon, S. Y. Yang, J. Byun and J. K. Kim, Electrically Actuatable Smart Nanoporous Membrane for Pulsatile Drug Release, *Nano Lett.*, 2011, **11**, 1284–1288.

115 Q. Ma, Y. Li, R. Wang, H. Xu, Q. Du, P. Gao and F. Xia, Towards explicit regulating-ion-transport: nanochannels with only function-elements at outer-surface, *Nat. Commun.*, 2021, **12**, 1573.

116 D. Zhang and X. Zhang, Bioinspired Solid-State Nanochannel Sensors: From Ionic Current Signals, Current, and Fluorescence Dual Signals to Faraday Current Signals, *Small*, 2021, 2100495.

117 Z. Sun, T. Liao, Y. Zhang, J. Shu, H. Zhang and G. J. Zhang, Biomimetic nanochannels based biosensor for ultrasensitive and label-free detection of nucleic acids, *Biosens. Bioelectron.*, 2016, **86**, 194–201.

118 M. Tsutsui, S. Ryuzaki, K. Yokota, Y. He, T. Washio, K. Tamada and T. Kawai, Field effect control of translocation dynamics in surround-gate nanopores, *Commun. Mater.*, 2021, **2**, 29.

119 Y. Ai, J. Liu, B. Zhang and S. Qian, Field Effect Regulation of DNA Translocation through a Nanopore, *Anal. Chem.*, 2010, **82**, 8217–8225.

120 Y. He, M. Tsutsui, C. Fan, M. Taniguchi and T. Kawai, Controlling DNA Translocation through Gate Modulation of Nanopore Wall Surface Charges, *ACS Nano*, 2011, **5**, 5509–5518.

121 M. Tsutsui, Y. He, M. Furuhashi, S. Rahong, M. Taniguchi and T. Kawai, Transverse electric field dragging of DNA in a nanochannel, *Sci. Rep.*, 2012, **2**, 394.

122 Y. Liu and L. Yobas, Slowing DNA Translocation in a Nanofluidic Field-Effect Transistor, *ACS Nano*, 2016, **10**, 3985–3994.

123 R. Ren, Y. Zhang, B. P. Nadappuram, B. Akpinar, D. Klenerman, A. P. Ivanov, J. B. Edel and Y. Korchev, Nanopore extended field-effect transistor for selective single-molecule biosensing, *Nat. Commun.*, 2017, **8**, 586.

124 R. Ren, X. Wang, S. Cai, Y. Zhang, Y. Korchev, A. P. Ivanov and J. B. Edel, Selective Sensing of Proteins Using Aptamer Functionalized Nanopore Extended Field-Effect Transistors, *Small Methods*, 2020, **4**, 2000356.